Charles University in Prague

Faculty of Science

Study program: Physical chemistry

Mgr. Michal Mazur

Chemistry of the Interlamellar Space of Two-dimensional Zeolites

Dissertation

Supervisor: Prof. Ing. Jiří Čejka, DrSc.

Prague, 2016

Univerzita Karlova v Praze

Přírodovědecká fakulta

Studijní program: Fyzikální chemie

Mgr. Michal Mazur

Chemie mezivrstvového prostoru dvojrozměrných zeolitů

Disertační práce

Školitel: Prof. Ing. Jiří Čejka, DrSc.

Praha, 2016

Prohlášení:

Na disertační práci jsem pracoval v oddělení Syntézy a katalýzy Ústavu fyzikální chemie J. Heyrovského, AV ČR, v.v.i.

Prohlašuji, že jsem závěrečnou práci zpracoval samostatně a že jsem uvedl všechny použité informační zdroje a literaturu. Tato práce ani její podstatná část nebyla předložena k získání jiného nebo stejného akademického titulu.

V Praze, 14. června 2016

Podpis

ACKNOWLEDGMENT

I wish to express my sincere thanks to my supervisor, Prof. Jiří Čejka, for giving me the opportunity to become a member of his research group at J. Heyrovský Institute of Physical Chemistry and to complete my thesis at the Czech Academy of Science. I am deeply grateful for his guidance, advices, and support given to me. I will always remember his invaluable help with gratitude.

I am deeply indebted to Dr. Wiesław J. Roth and Dr. Pavla Eliášová for their advices and many fruitful discussions that helped me to complete my work. I am grateful to Prof. Russell Morris and Dr. Paul Wheatley for outstanding cooperation and many suggestions essential for this contribution. I would like to express my very great appreciation to Prof. Petr Nachtigall and Mgr. Miroslav Položij for the theoretical calculations and modeling. I would like to thank Dr. Arnošt Zukal and Dr. Martin Kubů for nitrogen and argon adsorption measurements, Dr. Mariya Shamzhy and Dr. Maksym Opanasenko for remarkable advices and support. I would like to extend my thanks to all members of the Department of Synthesis and Catalysis for their priceless help and friendship.

Finally, I would like to thank to all my friends and family for encouragement and belief.

List of abbreviations:

ADOR	- assembly, disassembly, organization, reassembly
BET	- Brunauer-Emmett-Teller surface area
BSS1	- 1,4-bis-(triethoxysilyl)benzene
BSS2	- 1,2-bis-(triethoxysilyl)ethane
BSS3	- 4,4-bis-(triethoxysilyl)-1,1'-biphenyl
C_{16}TMA	- cetyltrimethylammonium chloride
DMP	- 2,6-dimethylpiperidine
DPA	- dipropylamine
DTA	- dodecyltrimethylammonium chloride
HMH	- hexamethonium bromide
HMTA	- hexamethylenetetramine
HRTEM	- high resolution transmission electron microscopy
IPC	- Institute of Physical Chemistry
IPC-1P	- two-dimensional layered precursor prepared by hydrolysis of **UTL** zeolite
IPC-1PI	- material prepared by pillaring of IPC-1SW
IPC-1SW	- IPC-1P intercalated with cetyltrimethylammonium cation
IPC-2	- three-dimensional zeolite with **OKO** topology
IPC-4	- three-dimensional zeolite with **PCR** topology
IPC-6	- three-dimensional zeolite alternating IPC-2 and IPC-4 layers
IPC-7	- three-dimensional zeolite alternating **UTL** and IPC-2 layers
IPC-9P	- two-dimensional layered precursor IPC-1P intercalated with choline or diethyldimethylammonium cation
IPC-9	- three-dimensional zeolite with 10-7-ring channel system
IPC-10	- three-dimensional zeolite with 12-9-ring channel system
IZA	- International Zeolite Association
LID	- local interatomic distance
LZP	- layered zeolite precursor
MAS NMR	- magic angle spinning nuclear magnetic resonance
NMP	- N-methylpiperidine
OA	- octylamine

OTA	- trimethyloctylammonium bromide
POS	- polyhedral oligomeric siloxane
POS1	- octakis(tetramethylammonium)T8-siloxane
SDA	- structure-directing agent
SEM	- scanning electron microscopy
SLC	- Sanders-Leslie-Catlow force field method
TA	- tributylamine
TEA	- tetraethylammonium bromide
TEOS	- tetraethyl orthosilicate
TET	- triethylenetetramine
TMA	- tetramethylammonium chloride
TMAA	- trimethyladamantylammonium hydroxide
TMPhA	- trimethylphenylammonium bromide
TPA	- tetrapropylammonium bromide
TPA-OH	- tetrapropylammonium hydroxide
UTL-H1	- hybrid material prepared of IPC-1SW intercalated with 1,4-bis-(triethoxysilyl)benzene
UTL-H2	- hybrid material prepared of IPC-1SW intercalated with 1,2-bis-(triethoxysilyl)ethane
UTL-H3	- hybrid material prepared of IPC-1SW intercalated with 4,4-bis-(triethoxysilyl)-1,1’-biphenyl
UTL-H4	- hybrid material prepared of IPC-1SW intercalated with octakis(tetramethylammonium)T8-siloxane
ε(B)	- extinction coefficient for Brønsted acid sites
ε(L)	- extinction coefficient for Lewis acid sites

List of publications:

The dissertation was completed based on the following publications:

1. M. Mazur, P.S. Wheatley, M. Navarro, W.J. Roth, M. Položij, A. Mayoral, P. Eliášová, P. Nachtigall, J. Čejka, R.E. Morris, *Synthesis of 'unfeasible' zeolites*, **Nature Chem.**, 8 (2016) 58-62

2. M. Mazur, P. Chlubná- Eliášová, W.J. Roth, J. Čejka, *Intercalation chemistry of layered zeolite precursor IPC-1P*, **Catal. Today**, 227 (2014) 37–44

3. M. Shamzhy, M. Mazur, M. Opanasenko, W.J. Roth, J. Čejka, *Swelling and pillaring of the layered precursor IPC-1P: tiny details determine everything*, **Dalton Trans.**, 43 (2014) 10548-10557

4. M. Mazur, M. Kubů, P.S. Wheatley, P. Eliášová, *Germanosilicate UTL and its rich chemistry of solid-state transformations towards IPC-2 (OKO) zeolite*, **Catal. Today**, 243 (2015) 23–31

5. P. Eliášová, M. Opanasenko, P.S. Wheatley, M. Shamzhy, M. Mazur, P. Nachtigall, W.J. Roth, R.E. Morris, J. Čejka, *The ADOR mechanism for the synthesis of new zeolites*, **Chem. Soc. Rev.**, 44 (2015) 7177-7206

6. M. Opanasenko, W. O. Parker Jr., M. Shamzhy , E. Montanari, M. Bellettato, M. Mazur, R. Millini, J. Čejka, *Hierarchical hybrid organic-inorganic materials with tunable textural properties obtained using zeolitic layered* precursor, **J. Am. Chem. Soc.**, 136 (2014) 2511–2519

7. R. L. Smith, P. Eliášová, M. Mazur, M. P. Attfield, J. Čejka, M. Anderson, *Atomic Force Microscopy of Novel Zeolitic Materials Prepared by Top-Down Synthesis and ADOR Mechanism*, **Chem. Eur. J.**, 20 (2014) 10446-1045

8. N. Žilková, P.Eliášová, S. Al-Khattaf, R.E. Morris, M. Mazur, J. Čejka, *The effect of UTL layer connectivity in isoreticular zeolites on the catalytic performance in toluene alkylation*, **Catal. Today**, in press, doi:10.1016/j.cattod.2015.09.033

Further publications:

9. H. Balcar, N. Žilková, M. Kubů, M. Mazur, Z. Bastl, J. Čejka, *Ru complexes of Hoveyda–Grubbs type immobilized on lamellar zeolites: activity in olefin metathesis reactions*, **Beilstein J. Org. Chem.**, 2015, 11, 2087–2096

10. M.V. Shamzhy, C. Ochoa-Hernández, V.I. Kasneryk, M.V. Opanasenko, M. Mazur, *Direct incorporation of B, Al, and Ga into medium-pore ITH zeolite: synthesis, acidic, and catalytic properties*, **Catal. Today**, in press, doi:10.1016/j.cattod.2015.10.013

Abstract

The presented PhD thesis is focused on the synthesis, characterization, and modifications of zeolites and zeolitic materials. The main interests are two-dimensional (2D) zeolites and modification of their interlamellar space. Presented work was performed at the Department of Synthesis and Catalysis at J. Heyrovský Institute of Physical Chemistry in Prague, Czech Republic under the supervision of Prof. Jiří Čejka.

Zeolites are inorganic crystalline solids with a microporous framework structure. They are widely used as catalysts, sorbents, and ion-exchangers. Conventional zeolites have been recognized as three-dimensional (3D) tetrahedrally-connected frameworks. However, some of them are also known to exist in various layered forms (2D zeolites). Recently, the transformation of 3D germanosilicate **UTL** into layers (IPC-1P) has started a new branch in 2D zeolites chemistry. This chemically selective degradation of **UTL** framework was performed via acid hydrolysis. In the structure of this germanosilicate, Ge atoms are preferentially located in specific building units, double-four-rings (D4R), which connect dense silica layers. Modifications of the layered precursor IPC-1P led to discovery of the two novel 3D zeolites: IPC-4 (**PCR**) and IPC-2 (**OKO**). This novel approach in the zeolite synthesis, called **ADOR** chemistry (**A**ssembly, **D**isassembly, **O**rganization, **R**eassembly), is in principle applicable to other germanosilicates with D4R units.

The thesis was focused on the investigation of the interlamellar space of 2D zeolite precursor – IPC-1P. The interlayer space was expanded by intercalation of organic compounds like amines and quaternary ammonium cations. The organic molecules organize the layers in designable way, e.g. with controlled interlayer distance. Calcination of variously intercalated precursor produces materials with substantial differences in the structure. This confirms that the use of various intercalates affects the organization of layers.

Intercalated IPC-1P precursor was subsequently modified either with silanes, alkoxysilanes, silsesquioxanes or polyhedral oligomeric siloxanes. Stabilization of IPC-1P with various silanes or siloxanes produces mostly IPC-2 zeolite, but also more expanded structures. It shows that the interlayer inorganic connections can be relatively short (e.g. one additional Si atom).

Expanded layers were connected with permanent props, which create large spectrum of novel materials with controllable textural properties. The interlayer distance of them was tuneable (expansion up to 35 Å). Amorphous silica props were introduced by pillaring procedure resulting in materials exhibiting BET areas and mesopores volumes up to 900 m^2/g and 0.6 cm^3/g, respectively. The incorporation of organic props (made of silsesquioxanes) resulted in hybrid organic-inorganic zeolitic materials. Final materials have relatively good thermal stability (up to 350 ^oC) and show BET areas and mesopores volumes larger than 1000 m^2/g and 1.0 cm^3/g, respectively.

The main aim of presented work was to produce new zeolites predicted by theoretical calculations. Theoretical studies suggested that there are millions of possible zeolite topologies. However, up-to-date only about two hundred were prepared by traditional solvothermal methods. The limitation of the synthesis of predicted zeolite frameworks is known as *zeolite conundrum*. Several criteria have been formulated to explain why most zeolites are unfeasible synthesis targets. Here, the procedure of the synthesis of two new zeolites is reported. Both of them were previously recognized as 'unfeasible'.

The novel materials were denoted as IPC-9 and IPC-10 and belong to the family of **ADOR** zeolites. These zeolites were obtained by reorganization of IPC-1P layers. Intercalation of proper organic molecules (choline, diethyldimethylammonium cation) at basic pH induces the shift of the layers to the preferable position. The layered precursor intercalated with choline or diethyldimethylammonium cation was denoted as IPC-9P. Direct condensation of IPC-9P creates new zeolite IPC-9 with higher framework energy than their unshifted analogue IPC-4. IPC-10 is formed by alkoxysilylation of IPC-9P. This new zeolite can be described as shifted analogue of IPC-2, with single-four-ring (S4R) units incorporated in between layers. New structures have exceptional channel systems exhibiting odd-member channels (10-7-rings and 12-9-rings for IPC-9 and IPC-10, respectively). Structures of IPC-9 and IPC-10 zeolites were confirmed using Rietveld refinement and Le Bail method by comparison of calculated XRD powder patterns with experimental ones. BET areas were 128 m^2/g and 217 m^2/g for IPC-9 and IPC-10, respectively. HRTEM images also proved the structure of new zeolites to be consistent with the predicted structural models.

The **ADOR** approach has been extended towards new synthetic pathway. The newly prepared zeolites have unprecedented energetics and rare structural features. The

results presented in the thesis show great opportunity for further exploration of this area and the possibility of preparing a whole new class of structures that cannot be accessed by traditional methods of synthesis. This study suggests that the *zeolite conundrum* is solved.

Abstrakt

Předložená dizertační práce se zabývá syntézou, charakterizací a modifikací zeolitů a zeolitických materiálů. Dizertace se zaměřuje především na dvourozměrné (2D) zeolity a modifikaci jejich mezivrstvového prostoru. Práce byla vypracována v Oddělení syntézy a katalýzy Ústavu fyzikální chemie J. Heyrovského AV ČR, v.v.i. pod vedením profesora Jiřího Čejky.

Zeolity jsou anorganické krystalické pevné látky s mikroporézní strukturou. Jsou široce využívány jako katalyzátory, sorbenty a iontoměniče. Obvykle jsou to třírozměrné (3D) struktury vzniklé propojením tetraedrů křemíku/hliníku. Některé zeolity existují také v různých vrstevnatých formách (2D zeolity). V nedávné době objev přeměny 3D germanokřemičitanu **UTL** na vrstevnatý materiál IPC-1P odstartoval novou oblast chemie 2D zeolitů. Ve struktuře tohoto germanokřemičitanu jsou atomy germania umístěny ve specifických stavebních jednotkách, tzv. double-four-ring (D4R), které tvoří pilíře mezi pevnými křemičitanovými vrstvami. Selektivní odstranění těchto D4R jednotek bylo provedeno pomocí kyselé hydrolýzy. Následná modifikace mezivrstvového prostoru prekurzoru IPC-1P vedla k objevu dvou nových 3D zeolitů: IPC-4 (**PCR**) a IPC-2 (**OKO**). Tento nový přístup přípravy nových zeolitů byl nazván **ADOR** (z anglického **A**ssembly, **D**isassembly, **O**rganization, **R**eassembly) a je v principu aplikovatelný na ostatní germanokřemičitany.

Hlavním tématem dizertace byl výzkum možných modifikací mezivrstvového prostoru 2D prekurzoru IPC-1P. Prostor mezi vrstvami byl zvětšen pomocí interkalace různých organických sloučenin (aminy a kvartérní amoniové soli). Vmezeřením organických molekul různých velikostí lze řídit vzdálenost mezi vrstvami. Po kalcinaci takto různě interkalovaných prekurzorů vznikají materiály s výrazně odlišnou strukturou. To potvrzuje, že interkalace rozdílných molekul ovlivňuje organizaci vrstev.

Interkalovaný prekurzor IPC-1P byl následně modifikován pomocí silanů, alkoxysilanů, silsesquioxanů nebo polyhedrálních oligomerických siloxanů. Stabilizací IPC-1P různými silany nebo siloxany vznikl převážně zeolit IPC-2, ale také struktury s více oddálenými vrstvami. To ukazuje, že nová anorganická spojení vrstev mohou být relativně krátká, tzn. o pouhý jeden atom křemíku větší.

Expandované vrstvy byly propojovány přes pevné můstky (pilíře), čímž vzniklo široké spektrum nových materiálů, u kterých bylo možné řídit jejich texturní vlastnosi a také vzdálenost mezi vrstvami (až na 35 Å). Vytvoření amorfních křemičitých můstků vedlo k přípravě materiálů se specifických BET povrchem až 900 m^2/g a objemem mesopórů až 0.6 cm^3/g. Zavedením organických můstků ze silsesquioxanů vznikly hybridní organicko-anorganické zeolitické materiály. Tyto materiály mají relativně dobrou termální stabilitu (do 300˚C) a vykazují specifické BET povrchy nad 1000 m^2/g a objemy pórů nad 1.0 cm^3/g.

Hlavním cílem předkládané práce byla příprava nových zeolitů předpovězených na základě teoretických studií. Teoretické práce naznačují, že by mělo být možné připravit miliony různých typů zeolitů. Přesto jich bylo dosud připraveno za použití tradiční solvotermální syntézy jen něco přes dvě stě. Toto omezení syntézy předpovězených zeolitů je ve vědě o zeolitech velká hádanka. K vysvětlení tohoto fenoménu bylo formulováno několik kritérií, které mají objasnit, proč je většina predikovaných struktur synteticky nedosažitelná. V této práci je popsána syntéza dvou nových zeolitů, které byly oba dříve považovány za „nedosažitelné“.

Nové materiály označené IPC-9 a IPC-10 patří do skupiny **ADOR** zeolitů a byly připraveny díky reorganizaci vrstev IPC-1P. Vmezeřením vhodných organických molekul (cholinu a diethyldimethylammoniového kationtu) za bazického pH dojde k posunu vrstev do požadované pozice. Vrstevnatý prekurzor interkalovaný cholinem nebo diethydimethylammoniovým kationtem se označuje jako IPC-9P. Přímou kondenzací IPC-9P vzniká nový zeolit IPC-9 s vyšší mřížkovou energií než má jeho analog s neposunutými vrstvami, IPC-4. Například zeolit IPC-9 je analogem zeolitu IPC-4, ale má posunuté vrstvy. Vzniká přímou kondenzací prekursoru IPC-9P. Zeolit IPC-10 vzniká alkoxysilylací IPC-9P prekurzoru. Tento nový zeolit může být popsán jako analog k IPC-2, kdy vrstvy jsou spojeny přes tzv. single-four-ring (S4R), ale v případě IPC-10 jsou vzájemně posunuté. Obě nové struktury mají výjimečné kanálové systémy s lichým počtem atomů tvořící vstup do kanálků (10-7-četné - IPC-9; 12-9-četné - IPC-10). Struktury IPC-9 a IPC-10 byly potvrzeny Rietveldovou a Le Bailovou metodou porovnáním experimentálních a simulovaných práškových rentgenogramů. Specifický BET povrch byl stanoven na 128 m^2/g pro IPC-9 a 217 m^2/g. Struktury obou zeolitů byly

potvrzeny i na základě HRTEM snímků, které jsou v souladu s předpovězenými strukturními modely.

ADOR metoda byla rozšířena o novou syntézní cestu spojenou s posunem vrstev. Nově připravené zeolity mají neobvyklé mřížkové energie a unikátní strukturní vlastnosti. Výsledky prezentované v předkládané dizertační práci poukazují na velké možnosti přípravy celé řady nových struktur, které nelze připravit klasickými syntézními cestami. Výsledky práce naznačují, že metoda ADOR umožňuje překonat dříve popsaná omezení hydrotermální syntézy zeolitů.

Outline

1. Aims of the study

This PhD thesis explores the chemistry of two-dimensional zeolites, their synthesis and modifications. Special interest was dedicated to the exploration of interlamellar space of zeolite precursor IPC-1P. The work was focused on searching of appropriate synthetic paths to prepare new materials, including fully crystalline zeolites. The main goals are summarized as follows:

Synthesis

- To investigate intercalation chemistry of IPC-1P zeolite precursor by introducing various organics into interlayer space.
- To prepare expanded zeolitic materials with designable textural properties by pillaring.
- To synthesise inorganic-organic hybrid materials based on IPC-1P layers.
- To synthesise computationally predicted zeolites IPC-9 and IPC-10 with unprecedented energy of the framework and rare, odd-ring channels.
- To extend ADOR approach as the alternative way of zeolite synthesis.

Characterization

- To perform detailed characterization of prepared materials using different techniques e.g. X-ray powder diffraction, nitrogen and argon adsorption measurements, and microscopy techniques (scanning and transmission electron microscopy).

2. Introduction

2.1. Zeolites

Zeolites are defined as crystalline microporous aluminosilicates with pores and cavities of molecular dimensions [1-4]. This class of inorganic materials is vastly used in catalysis [5-9], adsorption [10-12], separation [13-14], and ion exchange [15-16]. Recently, zeolites and zeolitic materials have found new applications in fields such as luminescence, medicine, electricity, microelectronics, and magnetism, etc. [17] Their widespread use in so many segments of science and technology is a consequence of their chemical composition and unique porous structures. Since the pioneering contributions by Barrer in 1940s [18], zeolites still remain in the spotlight of interest of many academic and industrial researchers worldwide. The continuous search for new zeolite topologies, their derivatives, and application of these materials is the source of many research papers in the most prestigious journals.

Zeolites are composed of TO_4 tetrahedra sharing corners. In this general formula, T stands for tetrahedrally coordinated framework atoms (usually Si and Al, but also other heteroatoms, such as B, Ge, Ti, Ga, etc.) [19]. Generally, zeolites are synthesized under the hydrothermal-solvothermal conditions [20]. The reaction medium typically consists of framework-forming atoms, solvent, structure-directing agent (SDA) and mineralizers (e.g. OH^- and/or F^-) [2, 21]. Most commonly, the synthesis generates three-dimensional materials, which crystallize directly from the reaction gel [22-24]. Even though the solvothermal approach is the most common for zeolites preparation it has some disadvantages. The biggest one for synthetic chemists is the limited control over the synthesis process and therefore, the structure of final product [25-26]. The mechanism of the formation of zeolites is still not completely revealed [20].As a result, most of the methodologies are based on trial-and-error approach. Nonetheless, the continuous study of this field brought several new strategies allowing a better control of zeolite synthesis towards materials with designed structures and specific features. Those strategies are based on the usage of pre-designed SDAs [27], topotactic transformation [28-29], heteroatom substitution [30], charge density mismatch [31], etc. Furthermore,

the development of theoretical methods such as structure determination or simulation techniques constantly increases the ability to solve complex zeolite structures and the prediction of hypothetical ones [32]. Improvement of theoretical and synthetic approaches caused rapid development in revelation of new zeolite topologies. Up-to-date, 231 framework type codes have been assigned by International Zeolite Association Structure Commission [33]. Surprisingly, this number is relatively low considering that computer enumeration suggests that there are millions of possible zeolite topologies [Fig 2.1] [34-37]. This is known as *zeolite conundrum* [38]. To explain it different feasibility criteria for successful synthesis of zeolites have been formulated [39-41]. Structures which do not obey these specific rules are not likely to be synthesized. The important question concerning this issue is: are these criteria ultimate and can one by-pass them to get beyond the currently suggested limits?

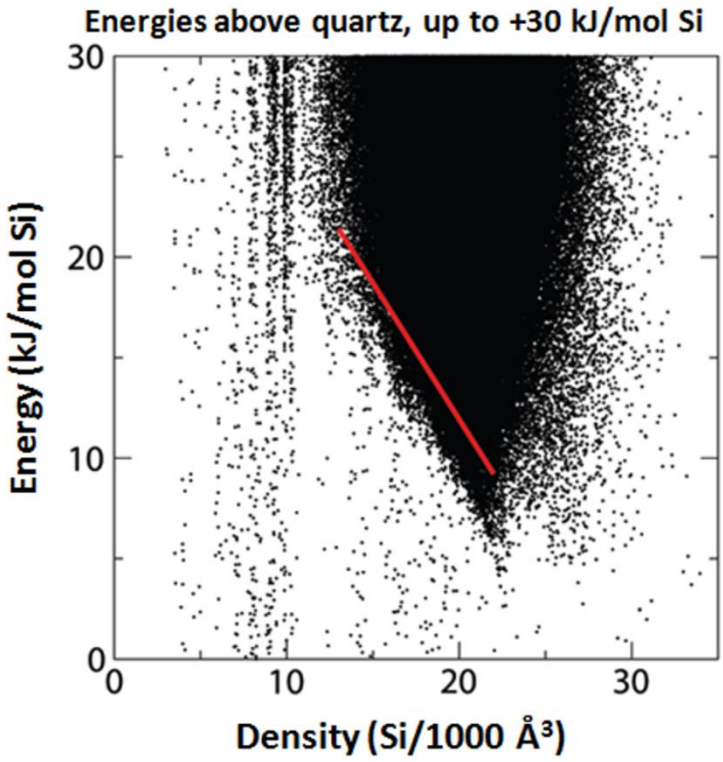

Fig. 2.1. Calculated possible zeolite structures. The red line shows the correlation presented by known silica zeolites, so-called traditional synthesis vector [34].

2.2. Feasibility of zeolite synthesis

Zeolite conundrum is based on the essential question: why have so few from all possible structures been made yet? To answer this question, criteria of the feasibility of zeolite synthesis have been proposed. These criteria include a measure of how far a hypothetical structure lies away from the energy-density correlation of zeolites that have already been synthesized. It is measured by a so-called feasibility factor ϑ [39], and the awareness that the known zeolites are usually placed in the certain range of density called the flexibility window [40]. The most recently formulated criteria are based on local interatomic distances (LIDs) and they assume that feasible zeolites are only those that obey these rules. It is described by limits on the values of the interatomic distances and angles [41]. These five geometrical criteria will be discussed below in detail (in unit 4.3.). All previously known zeolites obey all five LID criteria, so the ones that do not follow these rules were considered as "unfeasible".

It is commonly known that existing zeolites exhibit a strong correlation between framework energy and density. This dependence was predicted computationally [42-43] and also experimentally confirmed [44]. Regardless, theoretical studies have proposed relatively large set of hypothetical zeolites that do not show such a correlation. Those potential structures were postulated by connecting SiO_4 tetrahedra in every possible way. It resulted in the collection of hypothetical structures that cover a vast area in energy-density space [34] [Fig 2.1]. Noteworthy is the fact that all known zeolites can be found at the low-density edge of the energy-density distribution of this set of structures [34, 45]. This brings very important suggestion for synthetic chemists, that all known zeolites obey the correlation not because of properties of zeolites itself, but because of the kinetic limitations of the solvothermal synthesis procedure. In other words, most of the structures are considered as unfeasible to be prepared by conventional approach. Possible solution of this issue would be to find other synthetic pathways [46]. That brings us to the conclusion that development of new synthetic approaches could help to overcome the limitations of solvothermal synthesis and lead to preparation of zeolitic structures previously considered as unfeasible.

2.3. Synthesis of 3D and 2D zeolites and their modifications

The vast majority of zeolites are 3D structures synthesized via solvothermal method using different reaction conditions, reactants, and structure-directing agents [20]. Some zeolites can be obtained via solvent-free synthesis [47]. Despite the fact that in most cases the reaction proceeds directly to 3D zeolites, some zeolites were found to form two-dimensional (2D) layer zeolite precursors (LZP) [48-49]. 2D zeolites are materials with crystalline layers with thickness of a few unit cells at maximum. The lamellas are propagated in only two dimensions [28-29, 48, 50]. This kind of material combines the essential features of zeolites (like acidity) with the advantages of lamellas, i.e. overcoming the diffusion limits. Moreover, unlike the 3D zeolites, 2D zeolites have many post-synthesis modification possibilities. To date, 2D zeolites have been used for the preparation of the new materials via condensation, intercalation, stabilization, pillaring, and delamination processes. This resulted in more than 15 different structural types constructed with zeolite layers [51]. Most of them are not strictly zeolites due to the presence of additional non-4-connected components as consequence of the geometry of layers. Usually, the layers can be condensed into 3D solids, but not always to produce fully 4-connected materials. The examples of such zeolitic materials are Interlamellar Expanded Zeolites (IEZs) containing SiO_4 linkage connecting the layers [52].

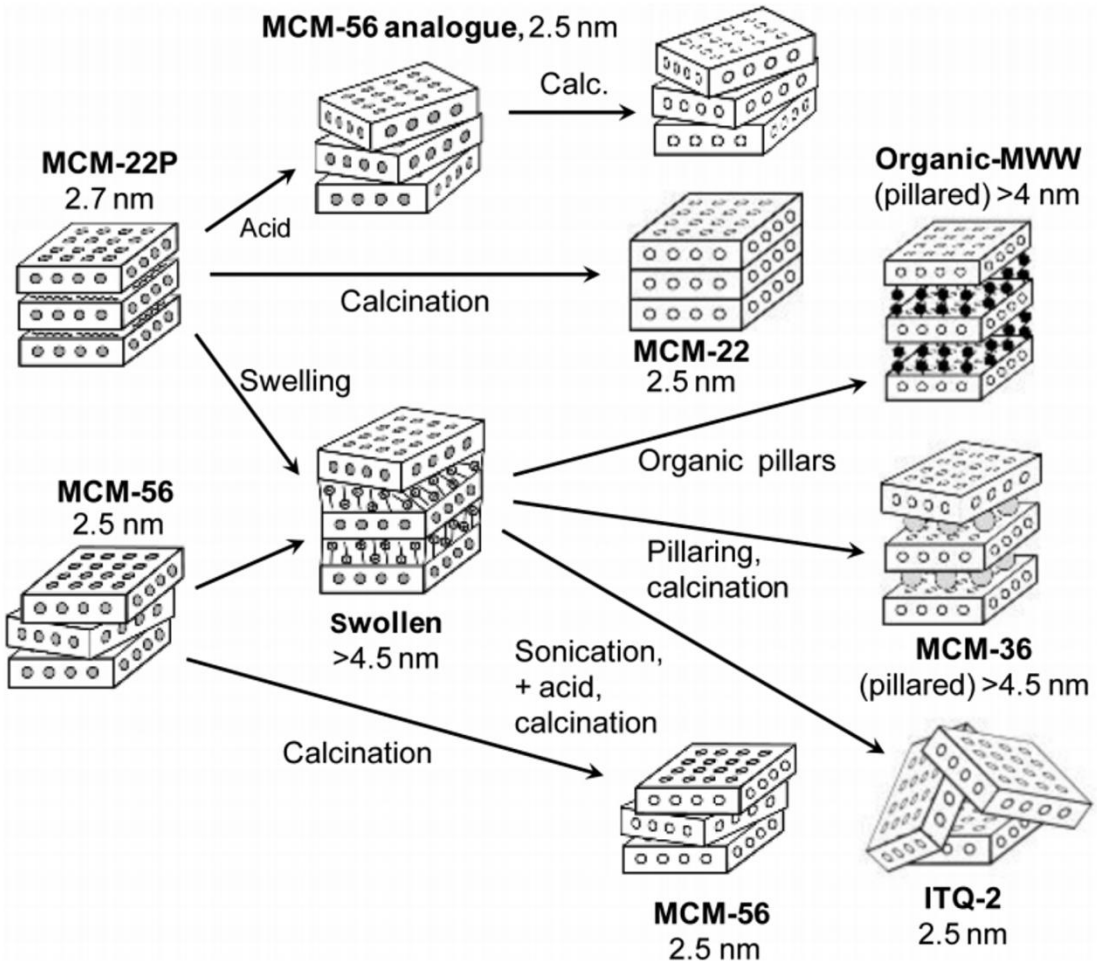

Fig. 2.2. Principal transformations reported for MCM-22P and MCM-56 with representative interlayer d001 spacing distances from XRD [53].

MCM-22P is one of the most important and explored 2D zeolites as - layered precursor with MWW topology [53-56] [Fig. 2.2.]. It has been shown that the synthesis of MWW can proceed along two different pathways: 1) direct synthesis, as in the standard zeolites (obtaining MCM-49) [55] or 2) via layered precursor (MCM-22P), which can be further calcined to 3D zeolite (MCM-22) [56]. The lamellar nature of MCM-22P was identified by the analysis of X-ray diffraction powder pattern. It shows the mixture of broad and narrow peaks; some of them underwent considerable shift toward lower d-spacing upon calcination. Pattern indexing confirmed the contraction of the unit cell in the *c* direction after calcination (about 2 Å). This was related to the condensation of surface silanol groups and formation of oxygen bridges between layers. The existence of MCM-22P layers was also proved by post-synthesis modifications like swelling and pillaring, which resulted in micro-mesoporous zeolitic material designated MCM-36

[54]. In most cases pillars are inorganic, exhibiting thermal resistance up to 500 ^{o}C and even higher. Moreover, for **MWW** layers the connections do not need to be necessarily inorganic. Pillaring with organic compounds has been carried out to combine advantages of solid structure of the inorganic zeolitic layers with easier and broader functionalization potential of organic pillars [57]. Main goal for producing this kind of materials is to attain high BET areas with much shorter diffusion paths in comparison with more condensed architectures like standard zeolites. Zeolite layers with **MWW** topology produce more than 10 different packing arrangements giving rise to a family of zeolitic architectures [58]. In principle this approach can be repeated with other frameworks. The zeolites of **AFO** [59], **AST** [60], **MTF** [61], **MWW** [58], **RRO** [62], **RWR** [63], and **SOD** [64] topologies as well as structurally related pairs having the same layers, but differently arranged, **CAS** [65] and **NSI** [66], **CDO** [67] and **FER** [68] have been obtained from directly synthesized 2D precursors. Most of these frameworks can also be synthesized by a direct route.

At the moment, there are two main direct ways to prepare 2D zeolites, both based on solvothermal procedure. First, it is the traditional direct synthesis analogous to the known methodology for discovering regular zeolites, such as the procedure for preparation MCM-22P - the first recognized layered zeolite [58] [Fig. 2.3.]. Second method, introduced by Ryoo and coworkers, was the synthesis of **MFI** nanosheets using specially designed SDA [69-70] [Fig. 2.3.].

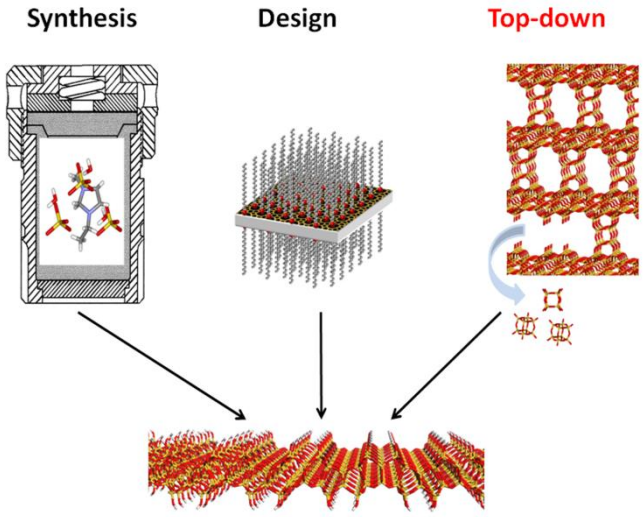

Fig. 2.3. The three main pathways for synthesis of two-dimensional zeolites [28].

Contrasting the traditional solvothermal synthesis, the topotactic transformation of zeolite frameworks has been developed as an efficient method for the preparation of new zeolitic materials. This strategy can be described as a solid-state structural transformation from one into another structure [71]. This is accomplished through various ways, e.g. dehydration-condensation [67, 72] or phase-to-phase reconstruction [73]. The example of synthesis by dehydration-condensation was described for silicate zeolite CDS-1 (**CDO**) prepared from layered silicate PLS-1 heated at high temperature under vacuum [67, 72]. Phase-to-phase 3D-3D reconstruction as an effect of pressure was shown by synthesis of ITQ-50 zeolite (**IFY**) from pure silica zeolite ITQ-29 (**LTA**) [73]. These methods can be used for preparation of new zeolite structures with predetermined units like layers, cages, or pores.

The most recently developed strategy in zeolite synthesis is **ADOR** approach (**A**ssembly-**D**isassembly-**O**rganization-**R**eassembly) [74-75]. This highly predictable method is based on the sequence of transformation steps whereby a previously assembled 3D zeolite is selectively and controllably disassembled into 2D layered zeolite precursor [Fig. 2.3.]. In the following steps, layers are organized into a suitable orientation and finally reassembled into a new, fully-connected, 3D zeolite, not possible to be prepared by solvothermal method by now [Fig 2.4]. ADOR method is universal and in principle can be employed for many zeolites, nevertheless, the first and the most thoroughly studied example of parent zeolite suitable for this purpose is germanosilicate **UTL**.

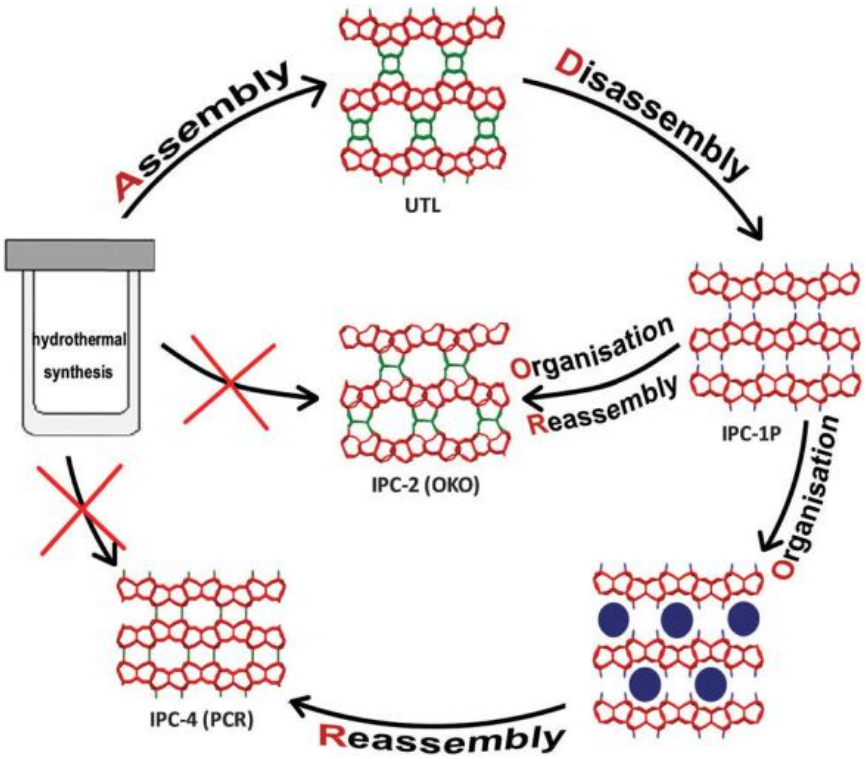

Fig. 2.4. The **ADOR** method scheme. **A**ssembly step is a hydrothermal synthesis of 3D **UTL** germanosilicate, **D**isassembly is hydrolysis of **UTL** to IPC-1P zeolite precursor, **O**rganisation is realized by intercalation of octylamine or dimethyldiethylsilane into IPC-1P, **R**eassembly is based on direct condensation or alkoxysilylation of IPC-1P to IPC-4 or IPC-2 respectively.

2.4. **UTL** as a parent zeolite for IPC materials family

Discovery of **UTL** zeolite was reported in 2004 independently by two research groups, designated as IM-12 [76] and ITQ-15 [77]. It was the first synthesized extra-large pore zeolite with intersecting 14- and 12-ring channels. The size of these pores is 9.5 x 7.1 Å and 8.5 x 5.5 Å, respectively. ITQ-15 was prepared using 1,1,3-trimethyl-6-azonia-tricyclo-[3.2.1.$4^{6,6}$]decane hydroxide as SDA. The template used for preparation of IM-12 was (6R,10S)-6,10-dimethyl-5-azoniaspiro[4.5]decane hydroxide. Further work exploring the formation of **UTL** zeolite showed that there are at least 21 organic compounds suitable as SDAs for the synthesis, all of them are spiro-azo compounds [78-79]. Moreover, the appropriate reaction mixture composition has to be used for producing desired structure. Final zeolites reported in the two initial papers had relatively low Si/Ge ratios: 4.5 and 8.5 for IM-12 and ITQ-15 respectively. Further investigation had shown that **UTL** formation is promoted in the case of lower Si/Ge

ratio, and without F^- anions in the reaction mixture [78-81]. **UTL** zeolite has been also exploited by incorporation of heteroelements into the structure. This was achieved by the optimization of synthesis parameters such as gel composition, pH, crystallization time, and so on. As result it was possible to gain **UTL** zeolite with Al, B, Ga, Fe, and In in the framework [80].

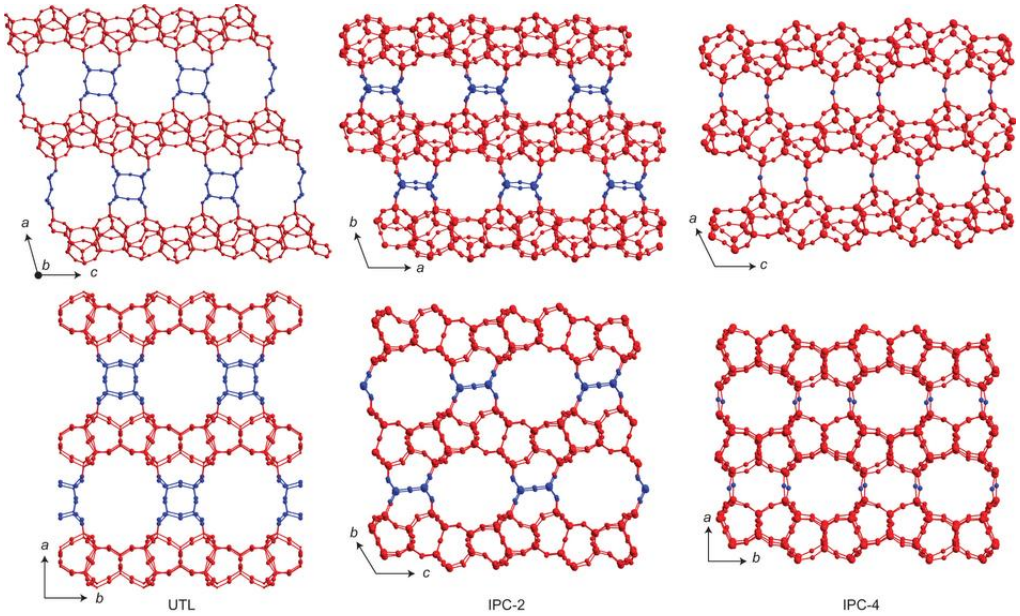

Fig. 2.5. Structural models of **UTL**, IPC-2 (**OKO**), and IPC-4 (**PCR**) zeolites [74].

UTL germanosilicate has been found appropriate for mentioned ADOR application because of its exceptional architecture. Generally, presence of the germanium atoms is known to promote the formation of double-four-ring units (D4Rs) [82-85]. The **UTL** structure can be described as compact silica layers connected with interlayer D4Rs. Those units consist mostly of Ge atoms. Not only the presence of Ge in double-four-ring is important, but also the number of these atoms in those units. D4R is cubic-shape unit consist of 8 T-sites. The Si/Ge ratio in the final **UTL** prepared by hydrothermal synthesis can vary in the range of 4.3 - 6.0. This means that the contribution of Ge in D4Rs can vary in the range of 7 Ge/unit (7Ge, 1Si) and 5 Ge/unit (5Ge, 3Si) respectively [86].

UTL zeolite substituted with heteroatoms was investigated in many catalytic reactions to take the advantage of its extra-large pore channel system [87-89]. Isomorphously substituted **UTL** zeolite with heteroatoms Al, Ga and Fe was tested in

disproportionation of toluene, toluene alkylation with isopropyl alcohol and trimethylbenzene disproportionation/isomerization [87]. Further investigated reactions were acylation of p-xylene with benzoyl chloride and Beckmann rearrangement of 1-indanone oxime [88]. Germanosilicates with various topologies (**UTL**, **BEC**, **UWY**, **IWR**) serve as efficient heterogeneous catalysts for the Baeyer–Villiger oxidation of ketones [89]. The issue in catalysis was the instability of the framework under certain reaction conditions. It appeared to be irreversibly damaged, especially in the presence of water [90]. As reported by Li et al. [91-92], zeolites become increasingly unstable in water with the proportional increase in the Ge content in the framework. The samples were so sensitive that the damage was caused even by atmospheric moisture. However, it was reported that the degradation of this structure can be controlled [75]. This was the breakthrough used for the introduction of novel synthetic strategy so-called ADOR approach [74].

2.5. ADOR process and staging chemistry

The assembly of 3D **UTL** zeolite is the first step of the ADOR approach. Second, disassembly step was possible to perform thanks to the instability of **UTL** structure. Zeolite was hydrolyzed in slightly acidic medium (0.1M hydrochloric acid or 1M acetic acid) resulting in its conversion to lamellar material [75]. Further analysis proved that during hydrolysis selective degradation of structure occurs. D4R units are selectively decomposed while dense silica layers are preserved. This distinctive process is possible because of essential differences in composition between layers and D4Rs. Apparently, the Si-O-Ge and Ge-O-Ge connections are less stable than Si-O-Si linkages, so it is possible to dismantle the 3D zeolite structure with simultaneous preservation of layers. The lamellar zeolite precursor obtained in this way was denoted IPC-1P [75].

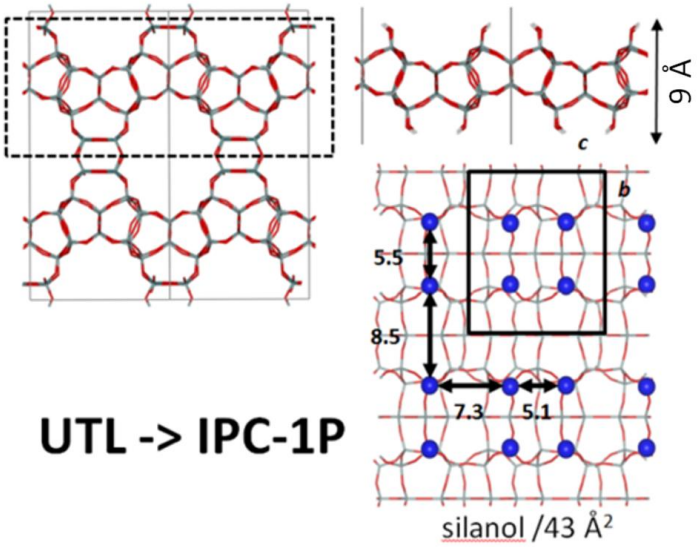

Fig. 2.6. Structure of 3D **UTL** zeolite, single IPC-1P layer, and silanol arrangement on its surface.

The thickness of a single **UTL** layer is approximately 9 Å and their x-y projection is the same like for pre**FER** layers [68]. IPC-1P and pre**FER** differ in the z-direction, as the IPC-1P have more complicated connectivity corresponding to longer repeat unit (12.5 Å, while for pre**FER** it is 7.5 Å). The relatively high stability of layers is probably the consequence of the lack of intralayer channels [75]. On the surface of layers there are silanol groups in the position where previously D4Rs were attached. The layers are not covalently bonded with each other; however they are connected by hydrogen bonds among surface silanols [93]. First attempts of the reconnection of the layers by calcination resulted in IPC-1 material, which presented rather poorly defined XRD pattern [Fig. 2.7.]. Presumably, the reconnection of layers by simple calcination occurs in not very organized way and IPC-1 consists of collapsed layers randomly connected with each other.

The theoretical investigation of IPC-1P layers brought the outcome that the specific location of the silanols on the surface of layers should allow to reassembly them in organized way to get new 3D zeolite [74]. Furthermore, the non-precedential location of surface silanols hypothetically permits four possible arrangements of layers to be reconnected to create four fully connected zeolites. This vision followed by the experimental investigation resulted in the discovery that IPC-1P intercalated with octylamine (OA) after calcination produces the well-organized structure, in fact one of

the four predicted zeolites. This material, denoted IPC-4, was proved to be four-connected zeolite with well-defined structure [74] [Fig. 2.5.]. This zeolite has the two intersecting channel system, perpendicularly crossing 10-ring and 8-ring, with size of 5.8 x 3.8 Å and 4.5 x 3.6 Å respectively. It was approved by Structure Commission of International Zeolite Association (IZA) with assigned code **PCR**. This realized the two final stages of ADOR strategy - organization of layers by using OA and reassembly them into new zeolite.

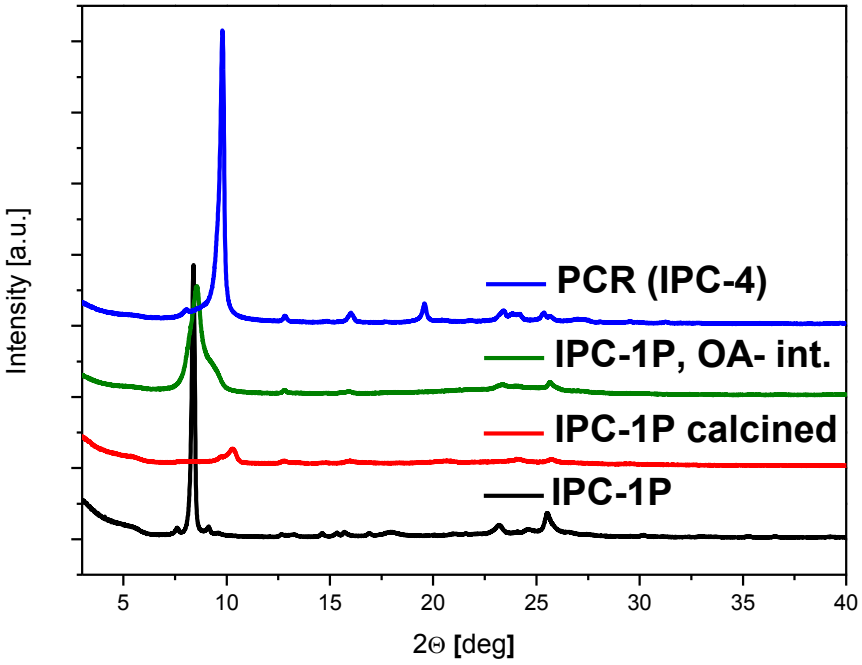

Fig. 2.7. The XRD powder patterns of IPC-1P layered precursor, IPC-1 calcined material, IPC-1P intercalated with octylamine, and **PCR** zeolite.

In conclusion to this, the accomplishment of idea of ADOR strategy has been done in four steps: assembly of **UTL** parent zeolite, its disassembly to IPC-1P layered precursor, organization of layers by intercalation of octylamine, and finally reassembly of intercalated precursor to another 3D zeolite – **PCR**.

Next zeolite prepared with ADOR was IPC-2, material isostructural to COK-14 [94] with **OKO** topology [Fig. 2.5.]. IPC-2 was prepared by the intercalation of silane-type molecules to the interlayer space of IPC-1P [74]. Similar procedure, so-called stabilization, was used for production of IEZs (e.g. for **MWW** topology) [95]. **MWW**-IEZ is not strictly zeolite because the interlamellar linkages are not fully connected with

each other [52]. By definition, atoms in the zeolite framework have to be fully 4-connected. Unlike the **MWW**-IEZ, stabilized IPC-1P was proved to be defined zeolite. Again, it was possible because of exceptional arrangement of surface silanols of IPC-1P. They are close enough to each other allowing the condensation of the linking silanes to create the single-four-rings (S4Rs) [Fig. 2.8.]. In other words, the IPC-2 zeolites consist of IPC-1P layers connected with S4R building units. This topology has intersecting 12-ring and 10-ring channels (6.6 x 6.2 Å and 5.4 x 5.3 Å, respectively). What is outstanding, at this point the ADOR shows that one parent zeolite (**UTL**) can be transformed to two different topologies (**PCR** and **OKO**).

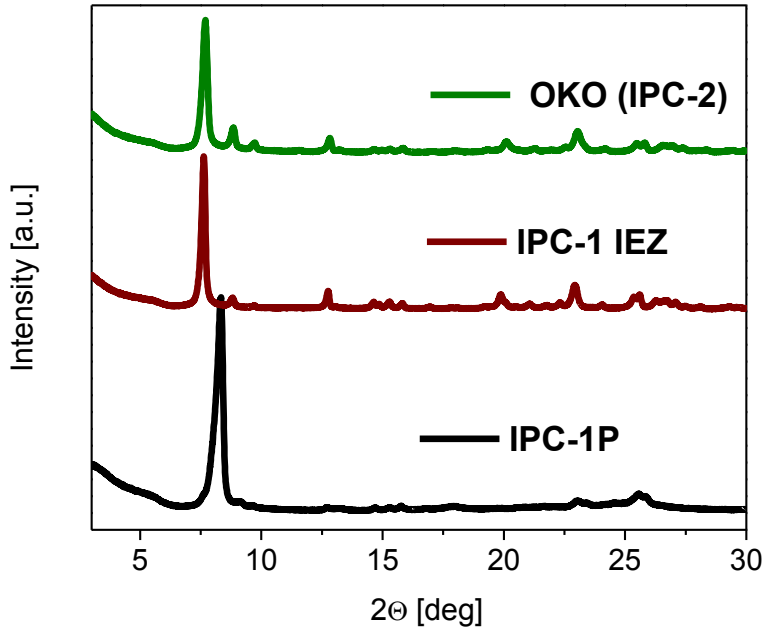

Fig. 2.8. XRD powder patterns of IPC-1P layered precursor, IPC-1 IEZ stabilized precursor, and **OKO** zeolite.

The synthesis of IPC-2 is the example of the organization of layers by intercalation of organizing agent finally covalently bonded to the layers. Beforehand, the synthesis of IPC-4 has shown that the organization of layers can be realized by intercalation of organics, which are SDA-type agents that order the layers through non-covalent interactions. Besides the intercalation mechanism of layers organization, the other technique was reported. It is based on self-organization mechanism. This type of process can have two possible outcomes depending which conditions were used: 1) de-intercalation of any residual species remaining between the IPC-1P layers followed by

alignment of them and 2) rearrangement of the silica within the layers to transfer into other part of framework and condensation into a different material. The study showed that employing different conditions e.g. various acidity, on calcined **UTL** samples changes the hydrolysis mechanism and final calcined samples have different interlamellar connections. Both, the presence and kind of the species between layers (oxygen bridges, S4Rs, and D4Rs) were found to be controllable during hydrolysis step depending on concentration of hydrochloric acid used, time, and temperature of treatment [96]. This study showed that there is linear relationship between the molarity of hydrolysis solution and d-spacing (d_{200}) as concentration increases up to 3M. Above this molarity the relationship is slightly more complex whereby at point of 5M HCl solution the d_{200} passes through maximum and then decreases as the concentration grows to 7M. Above 7M the d_{200} remains constant up to 12M. This phenomenon was described as the controllable degradation of structure. Following calcination produces materials with various ratios between interlamellar connecting species (D4Rs, S4Rs and oxygen bridges). This was claimed to be fully tuneable with two specific points of molarity. At first of them (1.5M) consecutive calcination creates the material with the same amount of oxygen bridges and S4Rs. The final material has two kinds of channel system 12-ring x 10-ring and 10-ring x 8-ring (can be described as alternating IPC-2 and IPC-4 layers; not an intergrowth of these topologies but new zeolite). This material was denoted as IPC-6. Second point of the molarity scale was found to be 5M, where, analogically to IPC-6, was recognized that 50% of connections are D4Rs and the other half are S4Rs. This material has two kinds of channel system 14-ring x 12-ring and 12-ring x 10-ring (can be described as alternating **UTL** and IPC-2 layers; again, not an intergrowth of these topologies but new zeolite denoted IPC-7). Overall, d-spacing of the final, calcined materials increases proportionally with the increasing acid concentration in the range from 0.01M to 5M. Under specific concentrations the well-ordered zeolites were obtained. Their d-spacing increases with following tendency: IPC-4 (0.01M) < IPC-6 (1.5M) < IPC-2 (3M) < IPC-7 (5M). Above the molarity of 5M the final solids were recognized as IPC-2 materials [96].

In the IPC family there are also materials with IPC-1P layers, which are not zeolites. The representative examples are swollen and pillared zeolites. Swelling, likewise in the **MWW** case [54], was performed by intercalation of hexadecyltrimethylammonium

(C_{16}TMA) cations into the interlayer space of precursor in basic environment (using tetrapropylammonium hydroxide solution - TPA-OH), and caused the expansion of the interlayer distance [97]. The obtained material was denoted IPC-1SW. Expanded precursor was used in consecutive pillaring process where tetraethyl orthosilicate (TEOS) was introduced in between IPC-1P layers. TEOS then was converted into amorphous pillars and calcined product was designated IPC-1PI [97]. This material, consisting of amorphous silica pillars supporting the IPC-1P layers, is of mesoporous structure with huge potential for catalytic applications.

As reported, IPC family is group of zeolites and zeolitic materials prepared from zeolite precursor by various post-synthesis modifications. The most interesting among them is ADOR process because of the great potential for synthesis of new architectures.

There are several great novelties in the ADOR approach. Namely, i) the first top-down synthesis of zeolite precursor, ii) the modification of one zeolite towards different topologies, iii) designable zeolite synthesis, iv) prospect of preparation of a set of zeolites with continuously tuneable porosity, etc. Current efforts of researchers still constantly increase the family of ADOR materials interesting from the structural and functional point of view [98]. In addition, **UTL** topology is not the only one 'ADORactive' and, in principle, described strategy can be extended to other germanosilicates, which make this method universal for synthesis of many new predictable zeolite structures [99].

In this contribution the chemistry of interlamellar space of 2D zeolite - IPC-1P is discussed. Presented research was mainly focused on the organization of layers by the intercalation of various molecules into IPC-1P. Extension of ADOR approach leading to two new zeolite topologies is presented.

3. Experimental part

Table 3.1. The list of chemicals used for syntheses and modifications.

Chemicals	Purity	Producer	Abbreviation
Cab-O-Sil M-5 (SiO_2)		Havel Composites	
Cetyltrimenthylammonium chloride	25 wt. % in H_2O	Aldrich	C_{16}TMA Cl
Diethoxydimethylsilane	98%	Aldrich	DEDMS
Germanium oxide	99,999%	Alfa Aesar	GeO_2
Tetraethyl orthosilicate	98%	Aldrich	TEOS
Tetrapropylammonium hydroxide	40 wt.% in H_2O	Aldrich	TPA OH
Hydrochloric acid	p.a.	Penta	HCl
1,4-bis-(triethoxysilyl)benzene	96%	Aldrich	BSS1
1,2-bis-(triethoxysilyl)ethane	96%	Aldrich	BSS2
4,4-bis-(triethoxysilyl)-1,1'-biphenyl	95%	Aldrich	BSS3
Octakis(tetramethylammonium)T8-siloxane		Aldrich	POS1
Sodium hydroxide	p.a. 98%	Penta	
Cis-2,6-Dimethylpiperidine	98%	Aldrich	
1,4-Dibromobutane	99%	Aldrich	
Aluminum hydroxide	Al_2O_3, 50-57%	Aldrich	$Al(OH)_3$
Acetic acid	99%	Aldrich	
Choline chloride	99%	Aldrich	
Diethyldimethylammonium hydroxide	20 wt. % in H_2O	Aldrich	

3.1. Synthesis and modifications of **UTL**-derivatives

Synthesis of the parent germanosilicate **UTL** was carried out under hydrothermal conditions. (6R,10S)-6,10-dimethyl-5-anizosporo[4.5]decane hydroxide was used as a SDA. Synthesis was performed following the procedure described by Shvets et al. [78]. The obtained bromide form of SDA was converted into hydroxide one by ion-exchange with AG 1-X8 resin (Bio-Rad). The yield of the product was about 93%. Structure of the SDA was confirmed by NMR spectroscopy [Fig. 3.1.].

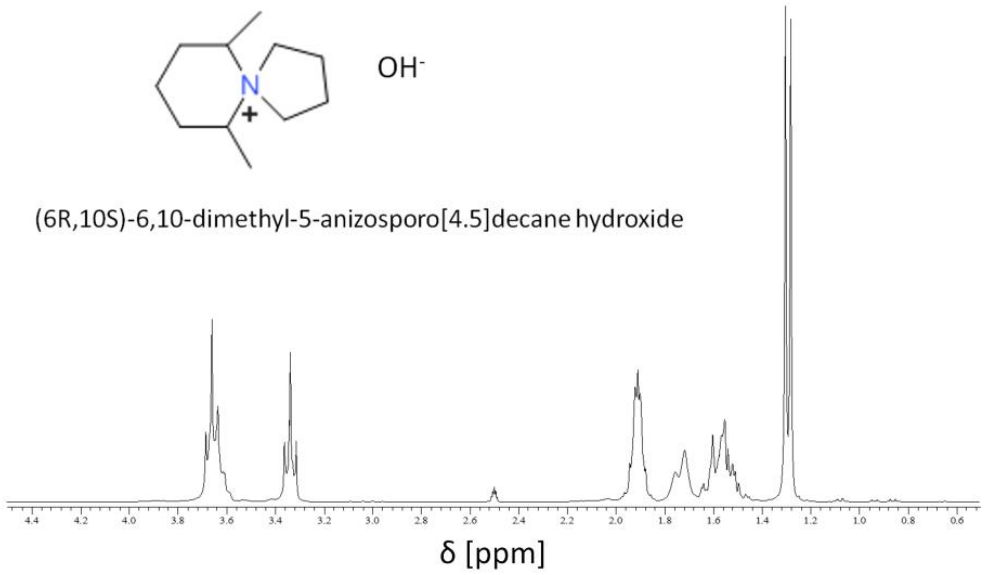

Fig. 3.1. The structural model of used SDA with ^{1}H NMR spectrum.

The reaction gel of a molar composition: 1.0 SiO_2: 0.5 GeO_2: 0.2 SDA: 37.5 H_2O was prepared by dissolving amorphous germanium dioxide (Aldrich) in the solution of SDA in water. Then, silica (Cab-O-Sil M5) was added into the solution and the mixture was stirred for 1h at room temperature. Al-containing **UTL** was prepared using aluminum hydroxide (Aldrich) as a source of Al. In case of Al-**UTL** the ratio of reaction mixture was: 0.782 SiO_2: 0.4 GeO_2: 0.018 $AlO_{1.5}$: 0.5 SDA: 30 H_2O. The obtained homogenous fluid gel was charged into 100 ml Teflon-lined autoclave and heated at 175 ^{o}C for 6 days with agitation (40 rpm). Synthesis of Al-**UTL** was performed for 28 days. The solid product was recovered by filtration, thoroughly washed out with distilled water and dried in the oven at 60 ^{o}C. To remove the SDA, the solid product was calcined in air at 550 ^{o}C for 6 h with a temperature ramp of 1 ^{o}/min.

3.1.1. Hydrolysis of **UTL**

Calcined **UTL** was hydrolyzed in 1M acetic acid with the w/w ratio 1/250 at 85 ^{o}C for 16 h. The product was isolated by centrifugation, washed with water and dried at 60 ^{o}C. The hydrolyzed product was a layered material denoted IPC-1P.

3.1.2. Intercalation of layered zeolite precursor

The layered material obtained by hydrolysis of **UTL** germanosilicate was treated with different amines or quaternary ammonium salts to attempt their intercalation between the layers. Used intercalates are collected in Table 3.2. Quaternary ammonium salts were prepared also in hydroxide form by ion-exchange following the procedure by Chlubná et al. [97]. The IPC-1P was treated with the solutions of the organic compounds with w/w ratio of 1/65 for 16 h. Intercalation of hydroxides was performed at room temperature. Amines and organic salts were introduced at 75 ^{o}C. The solid products were isolated by centrifugation, washed out with distilled water, centrifuged again, and dried at 60 ^{o}C. Intercalated layered precursors were denoted IPC-1P(organic). Samples were calcined at 550 ^{o}C for 8 h with a temperature ramp of 2 ^{o}/min.

Table 3.2. Organic agents used for intercalation of IPC-1P.

Organic agent	Abbreviation	Concentration in water [%]	Producer
Octylamine	OA	neat	Aldrich
2,6-dimethylpiperidine	DMP	neat	Aldrich
Triethylenetetramine	TET	neat	Aldrich
Dipropylamine	DPA	neat	Aldrich
Tributylamine	TA	neat	Aldrich
N-methylpiperidine	NMP	neat	Aldrich
Hexamethylenetetramine	HMTA	25	Aldrich
Hexamethonium bromide	HMH	25	Aldrich
Tetramethylammonium chloride	TMA	25	Aldrich
Tetraethylammonium bromide	TEA	25	Aldrich
Tetrapropylammonium bromide	TPA	25	Aldrich
Trimethylphenylammonium bromide	TMPhA	25	Aldrich
Trimethyladamantylammonium hydroxide	TMAA-OH	25	Sachem
Trimethyloctylammonium bromide	OTA	25	Aldrich
Dodecyltrimethylammonium chloride	DTA	25	Aldrich
Cetyltrimethylammonium chloride	C_{16}TMA	25	Aldrich

IPC-1P intercalated with choline hydroxide or diethyldimethylammonium hydroxide was designated as IPC-9P. Intercalation of those two molecules was performed in two ways: by direct intercalation and by de-swelling method. The first method, direct intercalation was achieved using 50% water solution of choline hydroxide. The choline hydroxide was prepared by ion-exchange of choline chloride 50% water solution using Ambersep® 900 resin (100 g of resin per 100 g of solution). Then, 1 g of zeolite precursor IPC-1P was mixed with 30 g of choline hydroxide solution and stirred for 4 h at room temperature. Measured pH of the mixture was 13. Solid IPC-9P was centrifuged, washed out with distilled water, centrifuged again, and dried in oven at 60 ^{o}C. De-swelling method involves an exchange of intercalate in between layers. The first step of the preparation was swelling of IPC-1P with C_{16}TMA-OH 25% solution with w/w ratio of 1/30 for 16 h at room temperature. Solid product was centrifuged, washed out with distilled water, and dried. Next step was choline-assisted de-swelling of swollen layered precursor (IPC-1PSW). A 0.62 g of IPC-1PSW was introduced into choline chloride (16 g) solution in absolute ethanol (40 g). The mixture was stirred for 10 h at room temperature, zeolitic powder was separated by centrifugation, decanted, washed once with absolute ethanol (~15 ml), and centrifuged again, then decanted and dried in oven at 60 ^{o}C. Repeating of the de-swelling ensures more complete exchange. IPC-9P was calcined at 550 ^{o}C for 8 h with temperature ramp of 2 ^{o}/min. The obtained material was designated as IPC-9. To get the IPC-9 zeolite with aluminum the Al-**UTL** was used as a parent material.

3.1.3. Alkoxysilylation

IPC-1P(organic)s were also stabilized by alkoxysilylation. The stabilization of intercalated IPC-1P was carried out in a 25 ml Teflon-lined autoclave. The reaction mixture contained 1.0 g of IPC-1P(organic), 10 ml of 1M HNO_3 water solution, and 0.5 g of diethoxydimethylsilane (DEDMS). The autoclave with reaction mixture was heated at 175 ^{o}C for 16 h. The solid product was separated by filtration, thoroughly washed with water, dried at 60 ^{o}C, and calcined. Calcination was carried out at 550 ^{o}C for 8 h with a temperature ramp of 2 ^{o}/min.

Synthesis of new zeolite IPC-10 was performed by alkoxysilylation of choline intercalated layered precursor. 0.1 g of IPC-9P was introduced to 25 ml teflon-lined autoclave. Then, 0.05 g of diethoxydimethylsilane and 10 ml of 1M HNO_3 was added. Autoclave was kept in the oven without agitation for 16 h at 175 ^{o}C. Product was filtered, washed with water (100 ml), and dried in oven at 60 ^{o}C. Final step was calcination at 550 ^{o}C for 8 h with temperature ramp of 2 ^{o}/min. Obtained product was designated as IPC-10. The IPC-10 samples containing aluminum had been prepared using Al-**UTL** as a parent material and additionally 0.1 g of $Al(NO_3)_3 \cdot 9H_2O$ was added to the autoclave in the alkoxysilylation step.

3.1.4. Pillaring

The pillaring of intercalated materials was carried out using 1 g of IPC-1P(organic) in 5 ml of TEOS. The mixture was stirred and heated under reflux at 99 ^{o}C for 16 h. The solid product was isolated by centrifugation and washed out with water (100 ml) for 8 h. After that, the product was once again isolated by centrifugation, washed out with water, dried at 60 ^{o}C, and calcined. Calcination was carried out at 550 ^{o}C for 8 h with a temperature ramp of 2 ^{o}/min.

3.1.5. Synthesis of zeolitic organic-inorganic hybrids

IPC-1SW (0.2 g) was vigorously stirred with a chloroform solution (5 ml) of 0.2 – 0.4 g of 1,4-bis-(triethoxysilyl)-benzene (BSS1), 1,2-bis-(triethoxysilyl)-ethane (BSS2), 4,4-bis-(triethoxysilyl)-1,1'-biphenyl (BSS3) or octakis(tetramethylammonium)T8-silsesqui-oxane (POS1) for 2 days at 60°C. Solvent was partially evaporated at 40°C and 20 torr. The white solid obtained was dried for 2 days at 65°C. To remove C_{16}TMA, the pillared material (0.2 g) was suspended in 30 ml of 1M NH_4NO_3 solution in ethanol/H_2O (w/w = 1/1) for 2 days at room temperature. The solid, separated by centrifugation, was treated with 0.2M HCl solution in ethanol/octane mixture (w/w = 1/1) for 2 days at 60°C. The final product was filtered off, washed with water, ethanol/octane (w/w = 1/1) solution, ethanol and then dried at 65°C overnight.

The materials obtained are denominated X**UTL**-HY, where X = w/w ratio for intercalating agent/IPC-1SW (1, 1.5, 2) and Y = 1 for BSS1, 2 for BSS2, 3 for BSS3 and 4 for POS1.

3.2. Characterization techniques

X-ray powder diffraction data were obtained on a Bruker AXS D8 Advance diffractometer with a Vantec-1 detector in the Bragg-Brentano geometry using $Cu_{K\alpha}$ radiation. Samples were gently ground using agate mortar to limit the effect of preferential orientation of individual crystals in the holder.

Textural parameters of the samples were determined using adsorption of nitrogen and argon. The adsorption isotherms of nitrogen at –196 °C and argon at –186 °C were recorded using an ASAP 2020 (Micromeritics) static volumetric apparatus. Before adsorption the samples were degassed under turbomolecular pump vacuum at 250 °C for 8 h.

The morphologies of the specimen particles were examined by scanning electron microscopy (SEM) using a JEOL JSM-5500LV. For the measurement, crystals were covered with a thin platinum layer by sputtering in vacuum chamber of a BAL-TEC SCD-050.

Concentrations of the Lewis (c_L) and Brønsted (c_B) acid sites were determined after adsorption of d_3-acetonitrile (ACN) and pyridine (PYR) by FT-IR spectroscopy using a Nicolet Protégé 460 Magna with a transmission MTC/A detector. The zeolites were pressed into self-supporting wafers with a density of 8.0 – 12 $mg \cdot cm^{-2}$ and activated in situ at T = 450 °C and p = $5 \cdot 10^{-5}$ Torr for 4 h. D_3-acetonitrile adsorption was carried out at room temperature (150 ^{o}C in case of pyridine) for 20 min at a partial pressure of 3.5 Torr, followed by desorption for 20 min at the same temperature. Before adsorption d_3-acetonitrile and pyridine were degassed by freezing-pump-thaw cycles. Spectra were recorded with a resolution of 4 cm^{-1} by collecting 128 scans for a single spectrum at room temperature, and then recalculated using a wafer density of 10 $mg \cdot cm^{-2}$. For a quantitative characterization of acid sites, the following bands and absorption coefficients were used: d_3-acetonitrile Brønsted band at 2296 cm^{-1} , ε = 2.05 $cm \cdot \mu mol^{-1}$, d_3-acetonitrile strong and weak Lewis bands at 2323 and 2310 cm^{-1} respectively , ε =

3.60 cm·μmol^{-1}. Concentration of c_L and c_B were evaluated from the integral intensities of bands at 1454 cm^{-1} and 1545 cm^{-1} respectively. The coefficients used were ε(L) = 2.22 cm·μmol^{-1} and ε(L) = 1.67 cm·μmol^{-1} [100].

^{13}C MAS NMR spectra were collected using an Agilent V-500 (at 126 MHz, 3.7 μs 90° pulse with a DEPTH filter [101], 30 s delay, spinal ^{1}H decoupling and shifts referenced to tetramethylsilane (0 ppm) using adamantane (at 38.5 and 29.4 ppm) for powders contained in 4 mm rotors spinning at 14 kHz. A Bruker ASX-300 was used to observe ^{29}Si (59 MHz, 3.8 μs = 60° pulse, 90 s delay, mlev16 ^{1}H decoupling, shifts referenced to tetramethylsilane at 0 ppm using tetrakis(trimethylsilyl)silane at -9.8 and -135.2 ppm) for samples contained in 7 mm rotors spinning at 5 kHz.

Thermogravimetric analyses were performed on a TG-750 Stanton Redcroft thermobalance in air between 20 and 900°C with a heating rate of 10°C/min. The weight of the sample was about 5 mg.

The thermogravimetric analyses and ^{13}C MAS NMR were performed in Eni S.p.A., Refining and Marketing Division, San Donato Milanese, Italy.

High resolution transmission electron microscopy (HRTEM) was carried out on a JEOL JEM-2011 electron microscope operating at an accelerating voltage of 200 kV. The HRTEM images were recorded using a 9 Gatan 794 CCD camera. The camera length, sample position, and magnification were calibrated using standard gold film methods. The measurements were carried out in Advanced Microscopy Laboratory, Nanoscience Institute of Aragon, University of Zaragoza, Spain.

4. Results and discussion

4.1. Expansion of the interlayer space

4.1.1. Separation of layers of IPC-1P

The first challenge was to propose the method how to control the interlayer distance of layered precursor. Hydrolysis of UTL zeolite under acidic conditions provides layered zeolite precursor denoted IPC-1P. It was recognized by the analysis of XRD powder patterns [Fig. 4.1.1.]. The dominant peak, indicating the interlayer distance, is shifted towards higher 2θ values. Moreover, the XRD pattern of IPC-1P shows intralayer reflections proving the preservation of layers [Fig. 4.1.1.]. This process is possible because of the presence of Ge atoms preferentially located in the D4R units in the zeolite framework. The bonds containing Ge atoms are less stable than those with silicon. Under acidic conditions (1M CH_3COOH, 85 ^oC) hydrolysis occurs. After hydrolysis only dense silica layers are preserved. On the surface of each layer there are silanol groups [Fig. 2.6.], which keep the layers together by hydrogen bonding. There are no covalent connections between separated layers, which makes possible to separate them during further modifications.

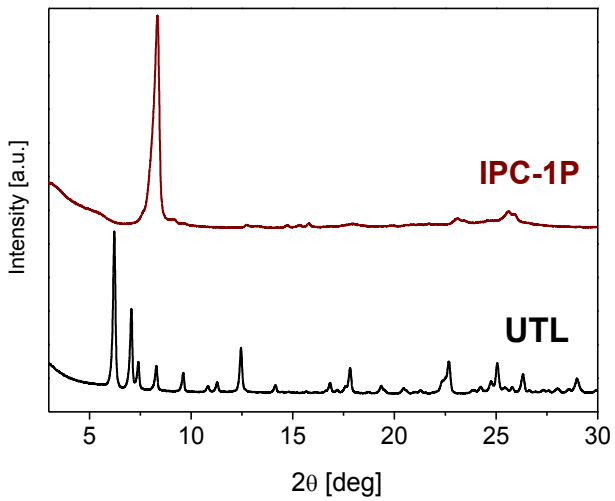

Fig. 4.1.1. XRD powder patterns of **UTL** zeolite (black) and IPC-1P layered precursor (red).

For the separation of the IPC-1P lamellas it is crucial to break the hydrogen bonds. The common way is to use the solution of intercalate with basic pH. The appropriate pH (pH approx. 13) was achieved by adding of a base (TPA-OH) or by exchange of the agent molecule itself to hydroxide form. Both routes were used in the study; however more regular materials were obtained by using the second method. Generally, diffraction lines were sharper and more intensive indicating better organization in the material. The major advantage of usage of exchanged organic agent is that there are no additional species in the system. Nevertheless, in some depicted processes the additional hydroxide solution had been used.

The next step was swelling. The purpose of swelling is an expansion of interlayer space of 2D zeolite. The standard agent used for swelling is hexadecyltrimethylammonium (C_{16}TMA) chloride or bromide in basic pH achieved by addition of TPA-OH. This procedure was successfully applied for IPC-1P.

Surfactants with different molecule size were used as swelling agents. General formula for used organics can be described as C_nTMACl, where n was the lenght of alkyl chain (n = 8, 10, 12, 14, 16, 18). The first strategy was the swelling with the mixture of chain surfactant solution and TPA-OH. Various size of the surfactant molecules was expected to influence the interlayer distance of expanded materials. XRD was used for determination of the interlayer distance [Fig. 4.1.2.B.]. Recorded XRD patterns showed dominant peaks in low-angle section. Position of these peaks (with Miller indexes (200)) corresponds with the distance between the layers of precursor. A series of peaks at higher angles located at 7–30^o 2θ are consistent with preserved intralayer peaks of UTL / IPC-1P proving unchanged structure of the layers [Fig. 4.1.1.].

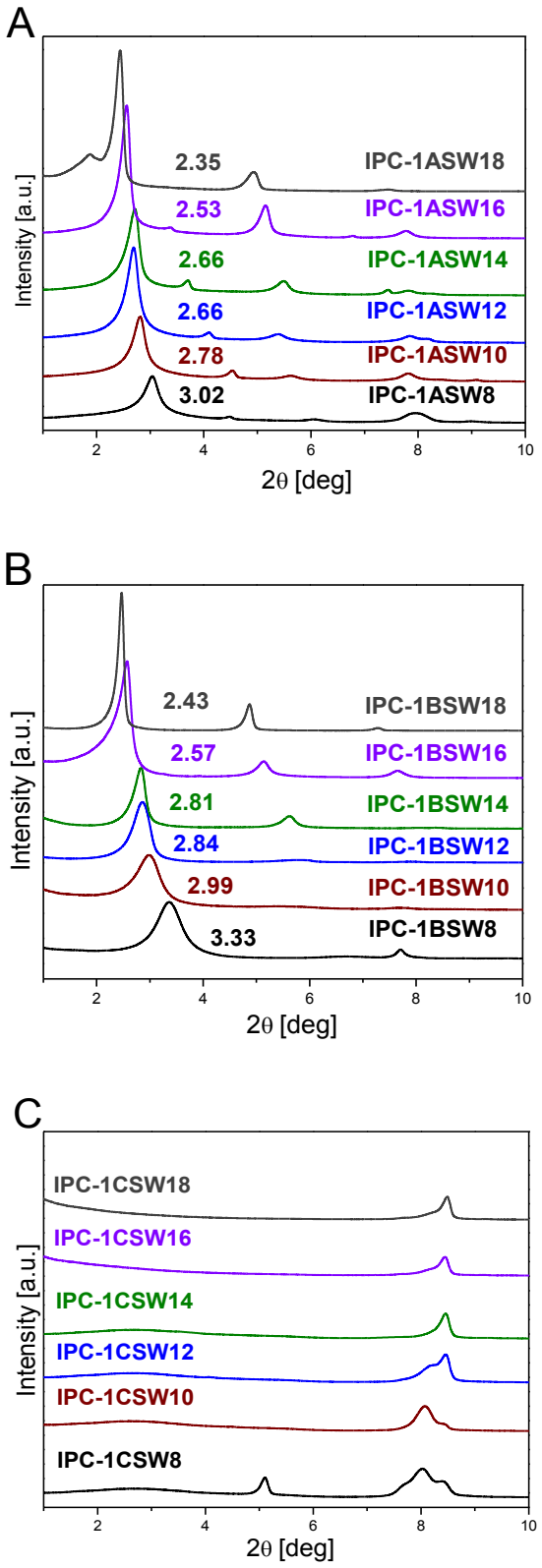

Fig. 4.1.2. XRD patterns of swollen samples obtained using C_nTMAOH at 25 °C (A), mixture of TPAOH and C_nTMACl at 25 °C (B), and C_nTMACl at 90 °C (C).

The second protocol involved the hydroxide form of surfactant instead of the chloride. This allows to avoid the introduction of TPA cations into the system [Fig. 4.2.1.A.], what presumably would increase the efficiency of swelling. Without additional TPA it is more likely that molecules of surfactant would be more packed in the interlayer space. Indeed, the XRD powder patterns of these materials proved this hypothesis [Fig. 4.2.1.A.]. The low-angle lines were slightly moved towards lower values with respect to previously described swollen materials (intercalated with the addition of TPA-OH) [Fig 4.2.1.B.]. Moreover, those peaks were sharper, which means that swelling with hydroxide form of surfactant produces more regular material. The interlayer distance in materials treated with hydroxide solutions increased with increasing length of the surfactant alkyl chain (18.6 (n = 8) < 21.1 (10) <22.6 (12) = 22.6 (14) < 24.3 (16) < 27.1 (18) Å). The swelling with surfactants in chloride form was not successful, and expansion was not observed [Fig. 4.2.1.], even at increased temperature (90 ^{o}C).

The next step was the treatment of the layered zeolite precursor IPC-1P with a series of amines and quaternary ammonium compounds with shorter chains. It was performed to investigate the influence of size and nature of the organic (guest) molecules on the interlayer distance in the intercalated product. Where possible, the treatments were carried out using neat liquids (amines), otherwise 25% aqueous solutions were used, sometimes in combination with added base to rise pH in order to enhance intercalation efficiency (especially in the case of introducing the cationic surfactants with long alkyl chains).

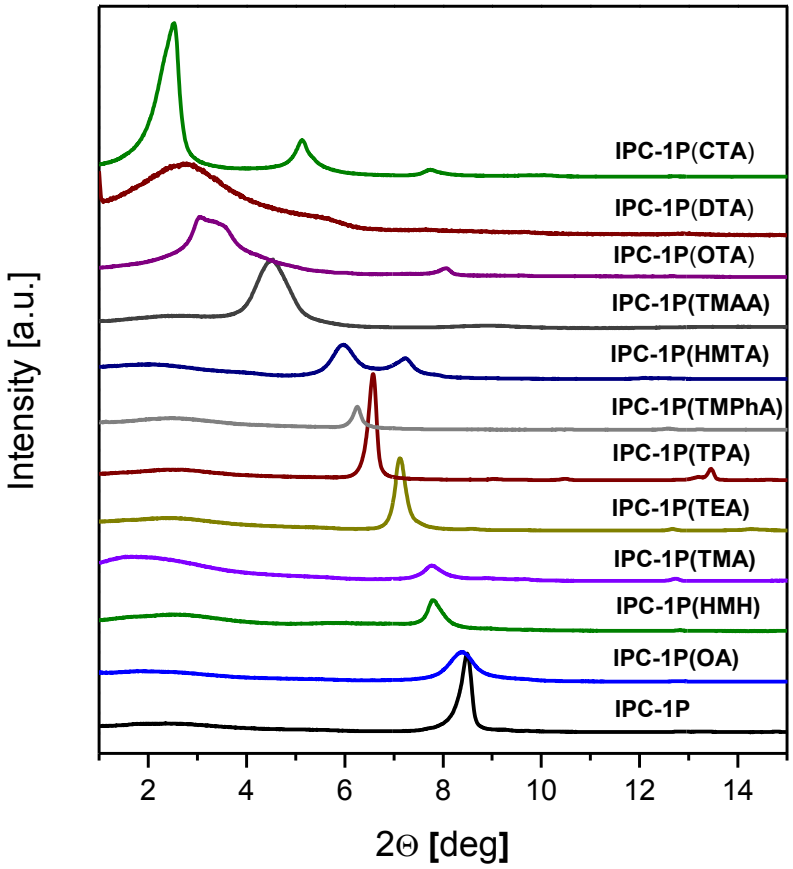

Fig. 4.1.3. XRD patterns of variously intercalated IPC-1P.

The treatments with amines and ammonium salts (chlorides or bromides) were performed at 75 ^{o}C while those at elevated pH (hydroxides) were performed at room temperature. Lower temperature in the case of hydroxides was used due to a sensitivity of IPC-1P layers to dissolution under basic conditions. The products designated IPC-1P(organic), were characterized by powder XRD [Fig. 4.1.3.]. Positions of the first dominant diffraction line, (hkl) = (200), correspond to the interlayer distance. It was confirmed that the size of the molecule is significant for the expansion the intercalation causes [Table 4.1]. Amines produce only a small expansion, which indicates the horizontal position of these molecules on the surface of the layered precursor [Fig. 4.1.4.]. Presumably, amines are not able to break the hydrogen bonding between individual layers and thus, the significant extension has not been observed.

However, even in the case of amines, the bigger intercalate is, the higher interlayer distance is produced.

This study showed that the interlayer expansion can be controlled by proper choice of intercalates. This opens further ground for another post-synthesis modification of expanded precursor.

Table 4.1. Interlayer d-spacing and calculated distances in intercalated IPC-1P.

Material	Organic agent	Low angle line, XRD		Distance extension
		2Θ [^{o}]	d-spacing	
IPC-1P	None	8.52	1.04	---
IPC-1P(OA)	Octylamine	8.42	1.05	0.01
IPC-1P(HMH)	Hexamethonium bromide	7.84	1.12	0.08
IPC-1P(TMA)	Tetramethylammonium chloride	7.80	1.13	0.09
IPC-1P(TEA)	Tetraethylammonium bromide	7.13	1.24	0.20
IPC-1P(TPA)	Tetrapropylammonium bromide	6.55	1.35	0.31
IPC-1P(TMPhA)	Trimethylphenylammonium bromide	6.25	1.41	0.37
IPC-1P(HMTA)	Hexamethylenetetramine	5.97	1.48	0.44
IPC-1P(TMAA)	Trimethyladamantylammonium hydroxide	4.53	1.95	0.91
IPC-1P(OTA)	Trimethyloctylammonium bromide	3.30	2.67	1.63
IPC-1P(DTA)	Dodecyltrimethylammonium chloride	2.80	3.15	2.11
IPC-1P(C_{16}TMA)	Cetyltrimethylammonium hydroxide	2.43	3.63	2.59

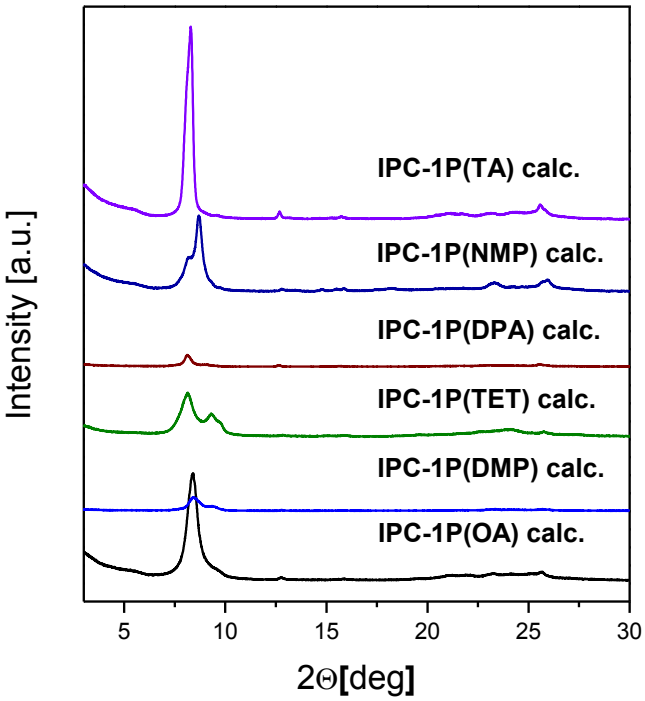

Fig. 4.1.4. XRD patterns for IPC-1P intercalated with amines.

Summarizing this part, the increase in the d-spacing upon intercalation compared with IPC-1P correlates with the size of intercalated organic molecules and expansion of the structure and varies from 1 Å for octylamine to 27.1 Å for the cationic surfactant with C_{18} chain. The high-angle diffraction peaks prove the preservation of silica layers of IPC-1P. The observed correlation between interlayer expansion and dimensions of intercalates indicates ability to control the former at least for the ranges studied. Intercalation is rarely the final goal and usually is the first step to further transformations.

4.1.2. Layers organization as a crucial step in ADOR approach

The ADOR approach is the synthetic strategy that has been successfully used for producing new zeolites. First zeolite prepared using ADOR protocol is IPC-4 zeolite (IZA code **PCR**). This zeolite is built of IPC-1P layers connected by oxygen bridges. Synthesis of this predicted structure was performed by the intercalation of octylamine into the

interlayer space of IPC-1P. As it was shown before, octylamine produces only minimal expansion [Fig. 2.7.]. This indicates that under the employed conditions molecules of octylamine are positioned horizontally on the surface of the layers. Even though the expansion caused by octylamine is very small, the presence of octylamine was crucial in producing the IPC-4 (**PCR**) zeolite.

The intercalation was followed by reconnection of the layers by oxygen bridges. To realize that IPC-1P(OA) was calcined in 550 ^{o}C for 8h. IPC-4, new 3D zeolite was the product of this process. What needs to be underlined, the calcination of pure, non-intercalated precursor usually did not produce a highly ordered zeolite but disordered IPC-1 material. It was concluded that octylamine is able to organize the layers of precursor. This hypothesis has been also proposed by theoretical study [74]. Moreover, theoretical investigation of the silanols on the surface of IPC-1P layers shows that there is more than one possible arrangement, in which the layers can be reconnected. In other words, if the layers would be organized and reassembled in a different way it would result in 3D fully connected zeolite different from IPC-4. According to the location of the surface silanols there are four possible ways to reconnect the IPC-1P layers. The calculations show that the most favourable arrangement due to the energetic factors is the one caused by intercalation of octylamine, in which the silanol quadruplets are directly one on another. Reassembly of layered precursor in this arrangement leads to **PCR** zeolite. Three other possibilities would require the shift of the layers towards different crystallographic axis and are much less energetically preferred. According to the theory, synthetic experience, and energetic rules for the solvothermal synthesis of zeolites those materials are not feasible to synthesize in standard way. Nevertheless those three structures were not likely to be obtained, the goal of this study was to find the conditions, under which the shift of the layers would be achieved.

Synthesis of IPC-4 zeolite proves that the intercalated organics are able to organize the layers in specific way to create ordered solids. Part 4.1.1. has shown that intercalation of organics can cause different expansion of the interlayer space. As a part of further characterization the samples of the intercalated products were calcined at above 550 ^{o}C. The organic guest molecules have been removed from the interlayer space. The corresponding XRD patterns show that the intercalating compounds were removed by

calcination, and layers covalently connected producing different materials depending on the nature of the organic. In most cases one either **PCR** (IPC-4) or **OKO** (IPC-2) were obtained. Generally, amines showed tendency to produce the smaller pore **PCR** of high quality, similar to that observed in the case of octylamine [Fig. 4.1.4]. It suggests that amines in general interact with hydrogen bonding present in IPC-1P in a favourable way for ordered condensation. Those results brings couple important conclusions. Firstly, it generalizes the outcome that was previously recognized with one compound only, i.e. octylamine, as intercalate. Secondly, it emphasizes the results of calculations about particularly favourable energy for one configuration of IPC-1P layers among four 4 possible, i.e. the one providing **PCR** zeolite. It also suggests that amines may not be good candidates to induce the remaining 3 alternative layers configurations leading to the other predicted zeolite structures. It should be reminded that calcination of IPC-1P without organic intercalates between layers produces material IPC-1 (d-spacing ≈ 8.8 Å) with poorly defined structure most likely due to lateral disorder (with no alignment of layers).

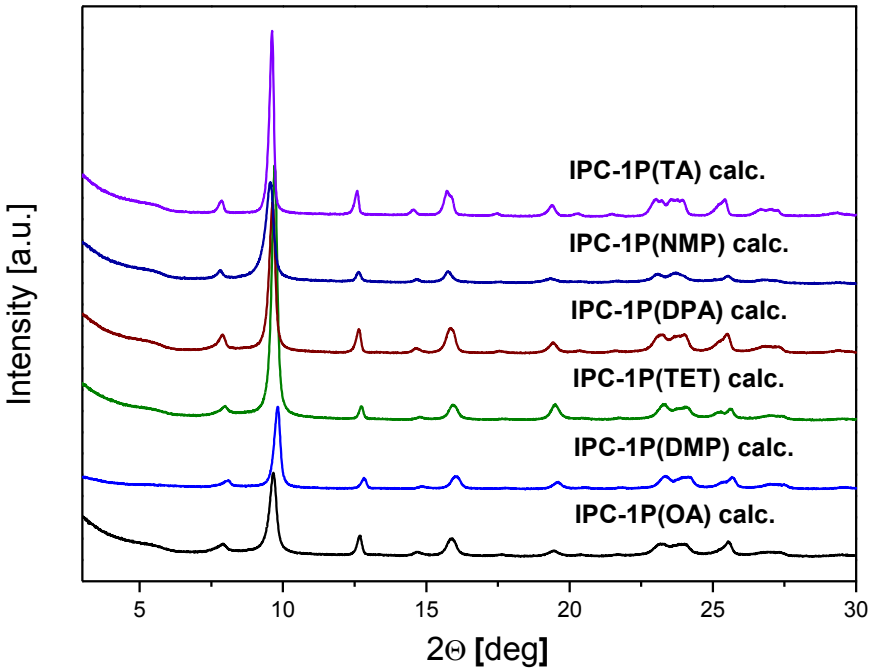

Fig. 4.1.5. XRD patterns for IPC-1P intercalated with amines, after calcination (550^{o}C).

Calcination of intercalated precursors with relatively large initial basal spacing gives inconclusive results [Fig. 4.1.6.]. XRD patterns suggest that IPC-1P(DTA) provides IPC-4 while calcination of IPC-1P(OTA) leads to a mixture of IPC-4 and IPC-2 zeolites. However, the calcination of IPC-1P(C_{16}TMA) and IPC-1P(TMAA), which also have large d-spacings, does not produce well-ordered materials. It can be recognized by very low intensities of diffraction lines. It resembles formation of IPC-1 and is probably caused by more expanded interlayer space (up to 27.1 Å) in those intercalated materials. During calcination process the intercalated organics were burned out. Presumably, long interlayer distance makes the organization of layers and formation of ordered, well-defined structures more difficult. It is also possible that pairs of each two layers may be fused as ordered units but across the crystal height there may be a mismatch in successive layers. The products observed after calcination of HMH, TMA, TEA and C_{16}MTA intercalated species resemble IPC-2, zeolite build of IPC-1P layers connected with S4Rs [Fig. 4.1.6.]. The formation of IPC-2 is partially seen also in the case of calcination of IPC-1P(OTA). As mentioned before, IPC-2 material is usually produced by stabilization procedure. Stabilization is based on addition of the source of silica (alkoxysilane) inserting silicate bridging moieties between layers. In this case no additional silica was used. This outcome is intriguing as it implies some kind of 'self-stabilization' process involving introduction of bridges that condense into the S4R units between layers. This requires additional free silica, which may come from partial decomposition and/or dissolution of the UTL layers during earlier treatments. The formation of stabilized structures without additional, separate alkoxysilylation has been reported before by Tatsumi et al. [95]. The novelty here is that it is achieved at basic pH while it is typically successful in rather strongly acidic medium.

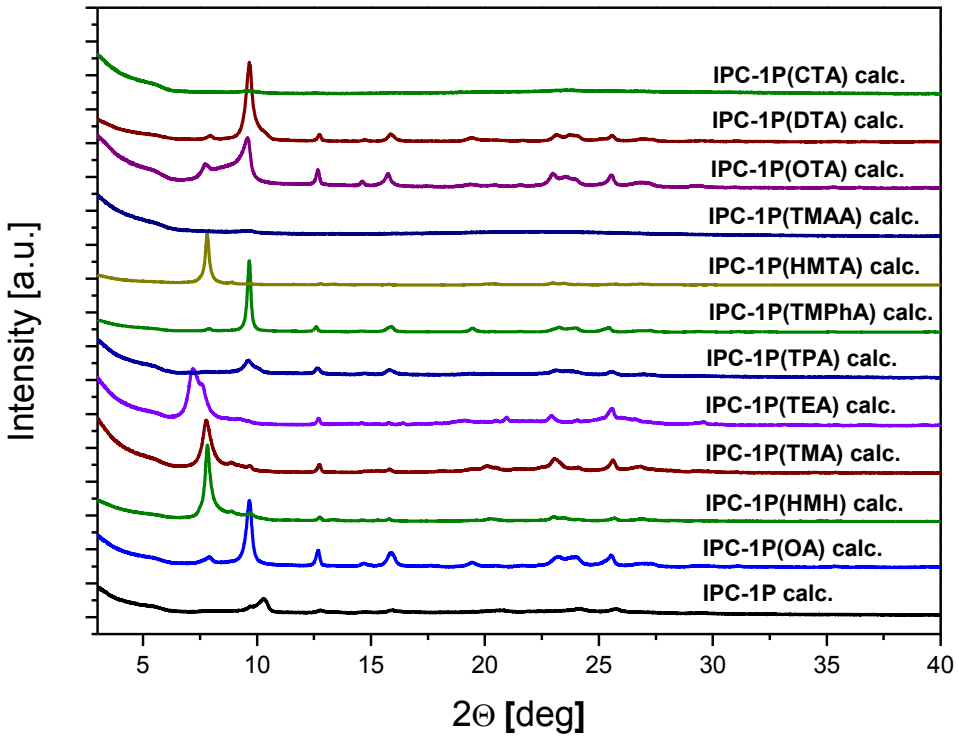

Fig. 4.1.6. XRD patterns for calcined IPC-1P and for variously intercalated IPC-1P after calcination (550^{o}C).

To conclude this part of the study, use of different organics as intercalates is fundamental for organization step in ADOR approach. Amines support the preparation of well-ordered IPC-4 zeolite. The surfactant molecules cause the bigger expansion of the interlayer distance, which is useful for further manipulations. However, calcination of relatively more expanded materials gives less ordered solids.

4.1.3. Props in the structure of 2D precursor

Layered zeolites can be modified by addition of props in between the layers. These props connect the consecutive layers and create three-dimensional framework of zeolite-based material. Props built into the structure can be of different types, inorganic [54] or organic [57], both type of materials were prepared with IPC-1P layers.

First example of introduction of permanent props is made with amorphous silica. This method, referred as pillaring, exploits inter-layer separation through swelling. In previous chapters, there has been shown that swelling can lead to the precursor with adjustable d-spacing (expansion of the structure up to 27.1 Å). The swelling of the latter followed by pillaring with appropriate silica source, TEOS, results in mesoporous molecular sieves with permanently expanded inter-layer distance.

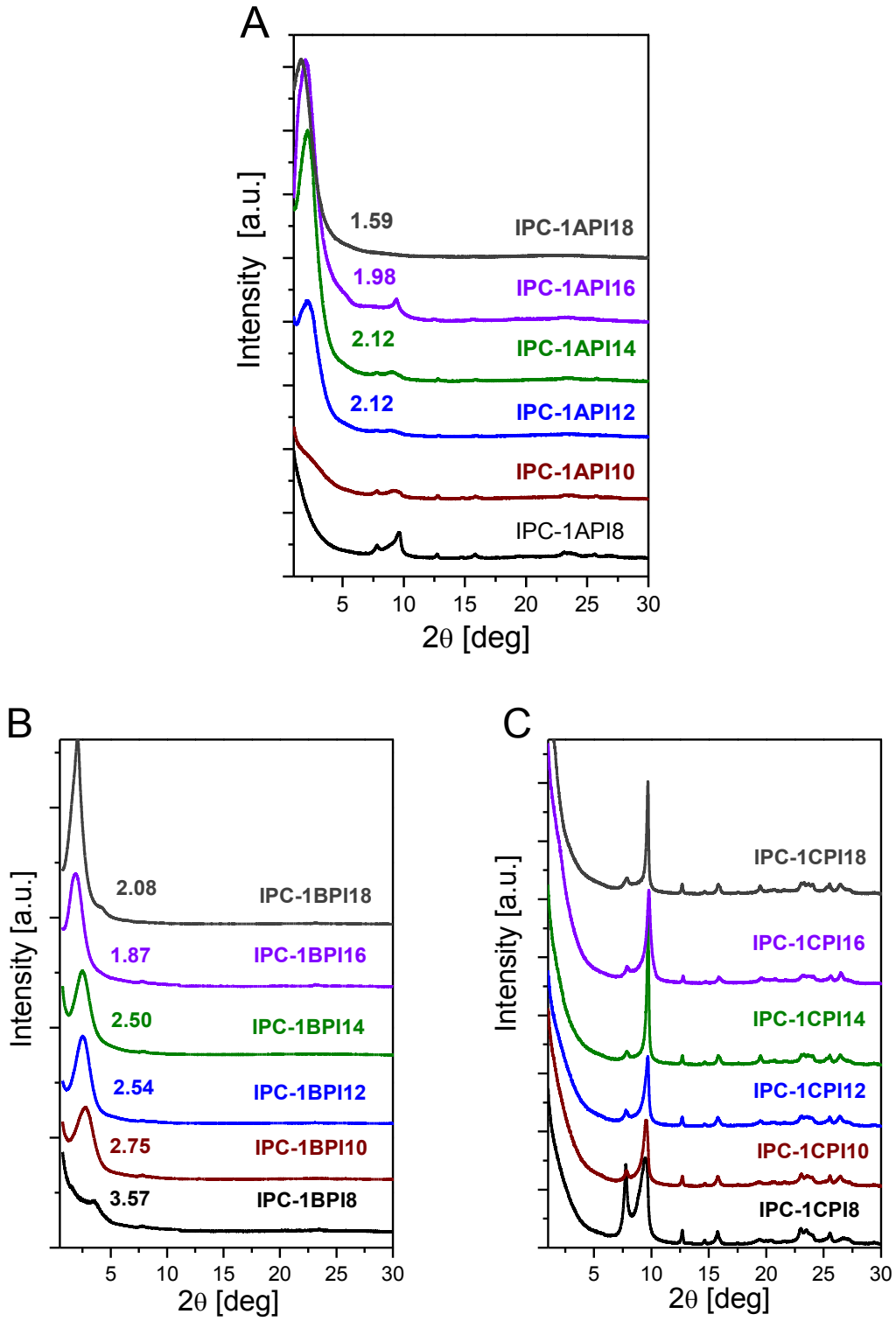

Fig. 4.1.7. XRD patterns of the pillared samples derived from samples swollen with the C_nTMAOH at 25 °C (A), mixture of TPAOH and C_nTMACl at 25 °C (B), C_nTMACl at 90 °C (C).

Based on the experience for pillaring of MWW layered precursor (MCM-22P) [54, 97] also IPC-1P has been investigated. The successful initial work on swelling and pillaring of IPC-1P was significant as the source of novel materials [75, 102]. The study of pillaring with TEOS was extended to IPC-1P intercalated (swollen) with various organic agents [Fig. 4.1.7., 4.1.8.]. It resulted in preparation of new mesoporous layered materials with adjustable textural properties.

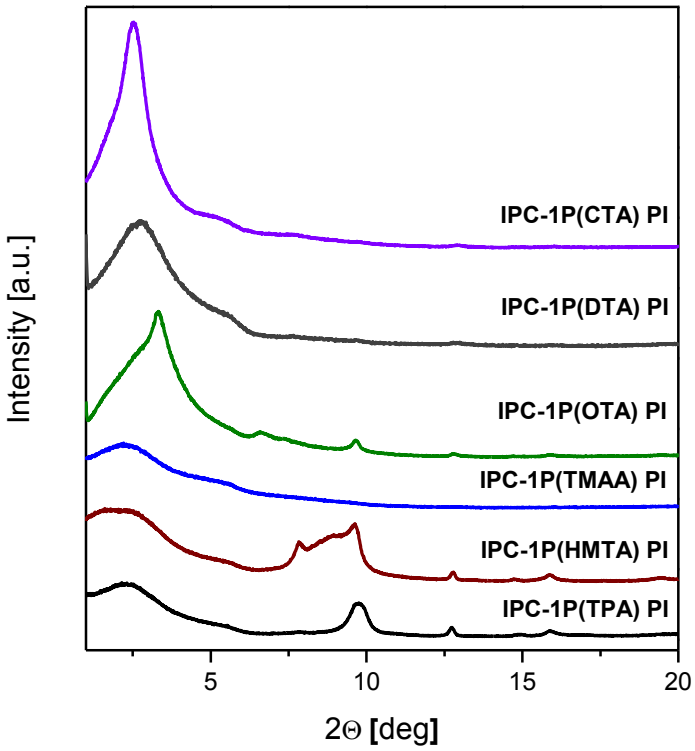

Fig. 4.1.8. XRD patterns for variously intercalated IPC-1P after pillaring procedure.

In opposite to MWW layers IPC-1P has no micropores. That is why pillared IPC-1P derivatives have no intra-layer microporosity. In other words, the layers are dense fragments of the framework. Adequate inter-layer distance is crucial for successful pillaring, which does not occur in the case of intercalated precursors with relatively d-spacing expansion less than 5 Å. This conclusion is based on the analyzed diffraction patterns and textural parameters measured by nitrogen sorption [Fig. 4.1.9.]. It is

probably due to constrained inter-layer space, most probably filled with organics preventing introduction of sufficient amount of silica in between layers.

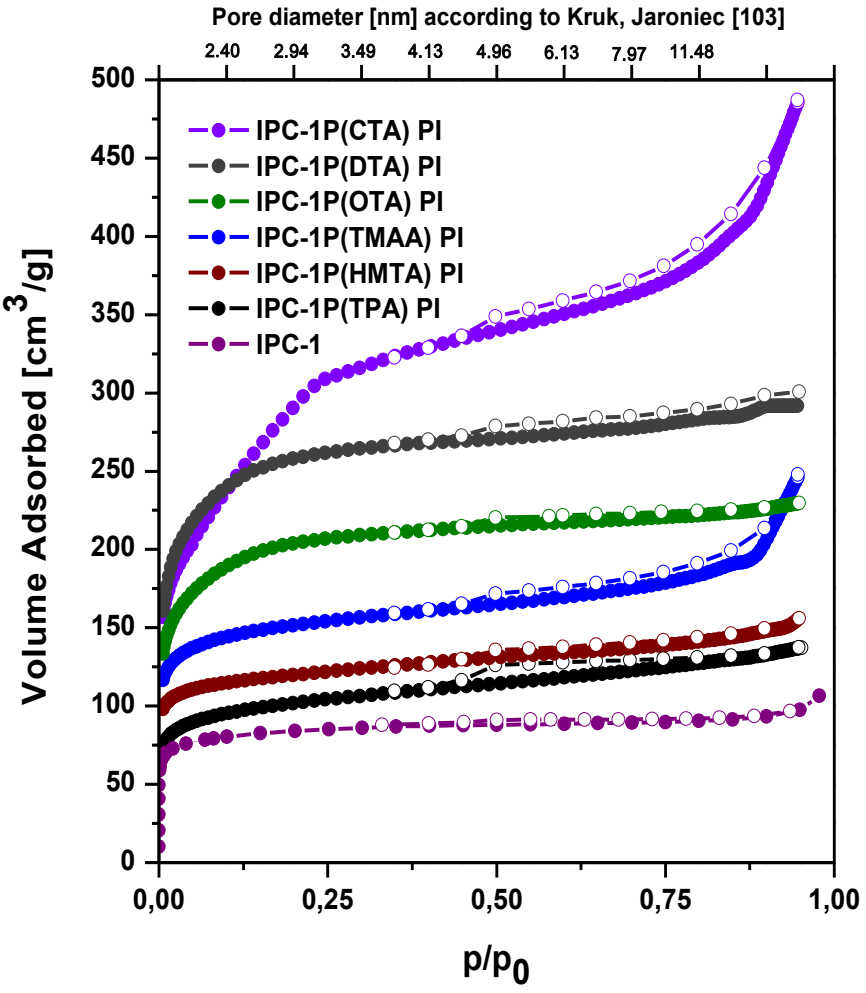

Fig 4.1.9. Nitrogen adsorption isotherms for IPC-1 and IPC-1P intercalated with TPA, HMTA, TMAA, OTA, DTA and CTA after pillaring procedure.
*Estimating pore size from nitrogen isotherm – values of the pore diameters calculated at selected nitrogen capillary condensation relative pressure [103].

Pillared derivatives of the samples swollen with mixtures of surfactants (CnTMA) and tetrapropylammonium hydroxide or tetraalkylammonium cations had a broader pore size distribution than those prepared using neat surfactant hydroxide (CnTMA-OH) solutions. The latter ones exhibited pore size distribution in the range of 25 – 35 Å. The pore size diameter of created mesopores corresponds to the dimensions of the correlative swelling agents and expansions gained using them. Another parameter

examined for its effect was the ratio of the pillaring agent TEOS in a chloroform solution to the swollen precursor. Optimal conditions were found to be TEOS/IPC-1P-swollen ratio = 1.5 (w/w). Pillared materials produced using this ratio had large BET areas and mesopores volumes (up to 900 m^2/g and 0.6 cm^3/g, respectively). As might be expected, too low amount of TEOS was not enough to create the well-ordered pillared derivatives. On the other hand, excess of TEOS resulted in decrease of the porosity [Fig. 4.1.10]. It indicates that pillaring using larger amount of TEOS creates thicker and densely distributed props.

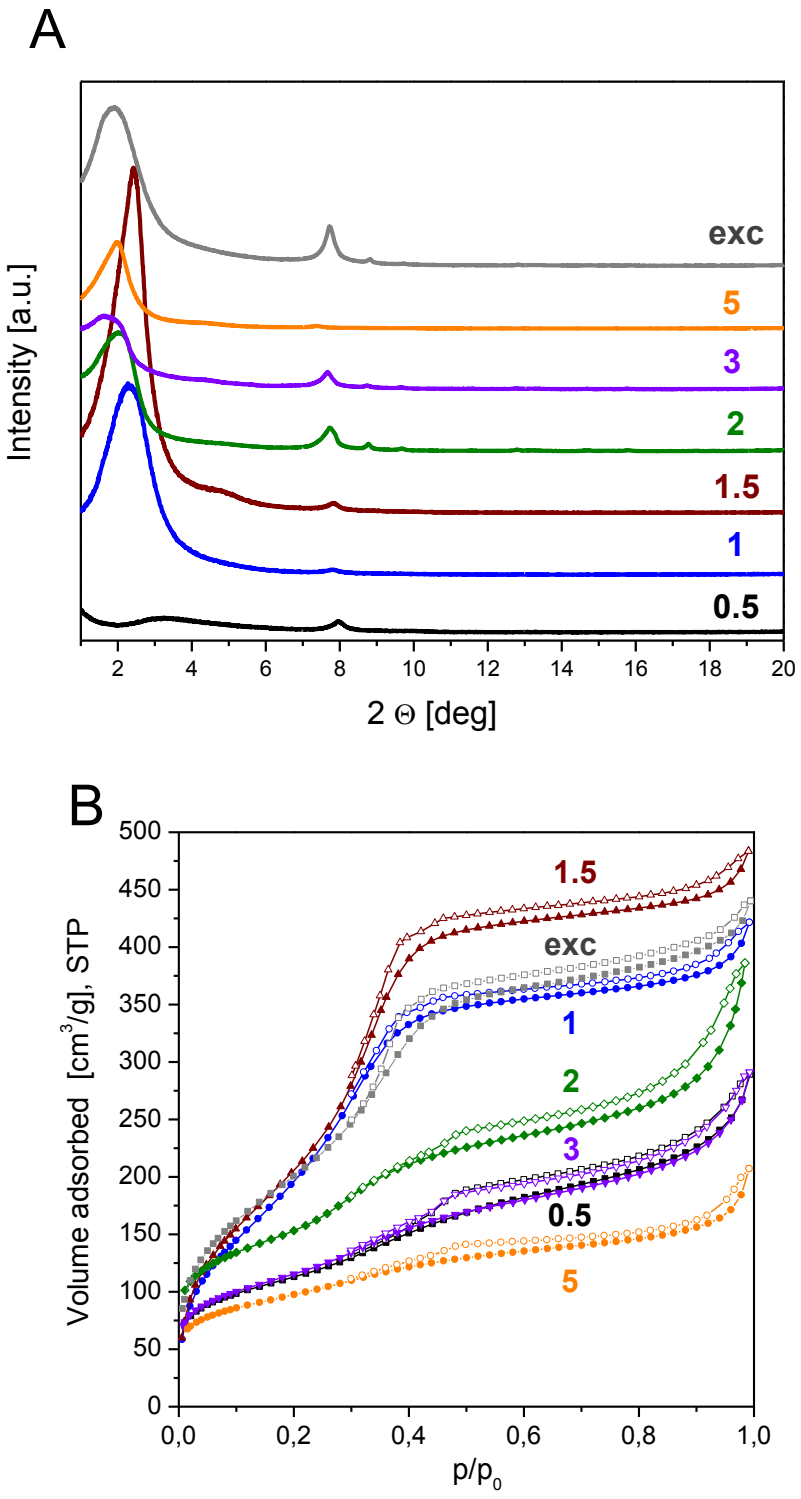

Fig. 4.1.10. XRD patterns (A) and Ar ad-/desorption isotherms (-186 °C) (B) for the pillared samples with different TEOS / IPC-1BSW16 ratio obtained using C_{16}TMAOH at 25 °C followed by calcination.

The inorganic connections in between the layers do not have to be amorphous. In case of using alkoxysilanes as intercalates it is possible to build 3D zeolite from IPC-1P layers. It is realized by incorporating additional silicon atoms between layers. As mentioned before, this so called 'stabilization' process results in Interlamellar Expanded Zeolite. It is more open than directly condensed (by calcination) layers. The typical stabilization procedure of zeolite precursor is based on alkoxysilylation with diethoxydimethylsilane in acid solution followed by calcination at 550 ^{o}C in the air to remove the organic residue. As found previously, the stabilized IPC-1P is unique among the other precursors because the distribution of the silanol groups on the surface of layers. They create silanol nests consisting of 4 groups close to each other. The silanol density in the case of IPC-1P is relatively high (1 silanol/43 Å^2) [74] in comparison with other zeolite precursors, e.g. MCM-22P has 1 silanol/ 90 Å^2 [104]. Thus, after the stabilization, interlayer siloxane bridges are close enough to each other to condense producing square S4R units between layers. Therefore, differently from other zeolite topologies, stabilization of IPC-1P leads to the fully connected, 3D zeolite - IPC-2 (OKO). Structure of this zeolite with S4R interlayer units is in between IPC-4 (layers connected by oxygen bridges) and UTL (layers connected with D4R units) in terms of interlayer distance. The variously intercalated precursors were subjected to stabilization. Majority of the IPC-1P(organic) materials, especially those with smaller organic, did produce IPC-2 as the final product. However, stabilization of initially more expanded precursors leads to obtain structure with longer interlayer distance [Fig. 4.1.11].

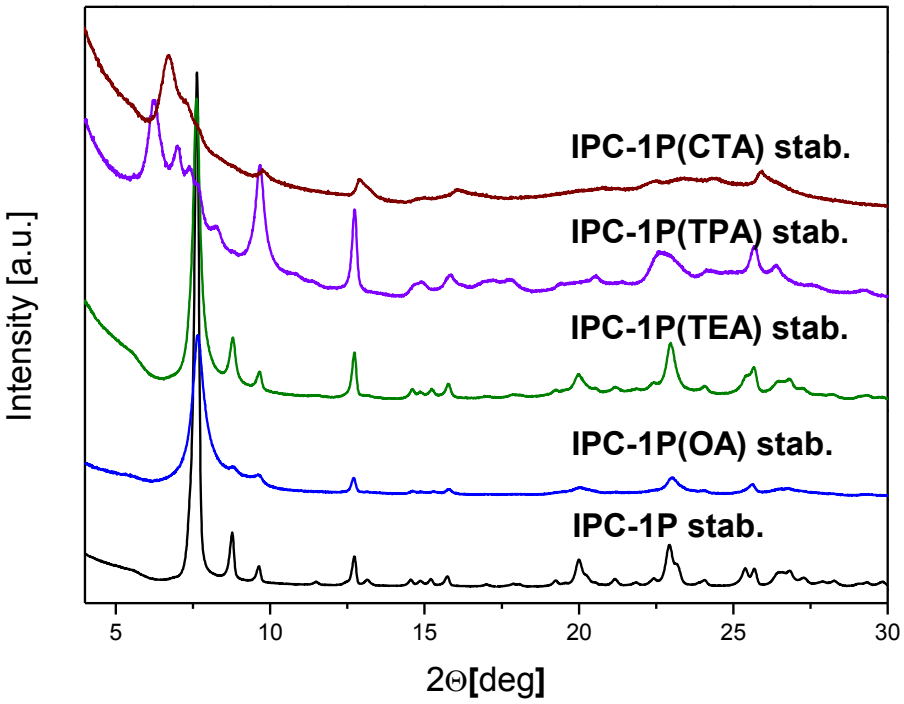

Fig. 4.1.11. XRD patterns for stabilized IPC-1P and IPC-1P intercalated with OA, TEA, TPA and C_{16}TMA after stabilization procedure.

This was concluded based on similarity of the XRD patterns positions of the most intense maximum corresponding to d = 11.5 Å. Some of the intercalated precursors, particularly those with larger organic agents like TPA and C_{16}TMA, seemed to produce more expanded structures. It is determined based on the presence of peaks at lower 2Θ[°] values (6.24 and 6.68 respectively) than IPC-2. XRD patterns for these materials have several additional peaks in the range from 6.2 to 8.1 [°], which may indicate mixtures of differently expanded structures, rather than single components. Those materials were not fully described yet, but they look promising and should be further explored. Perhaps, firstly by attempt to enrich the content of the expanded phase. As is typical for this kind of chemistry separation of each phase included in this mixture is hardly possible, that is why the effort should be directed towards obtaining separate well-ordered phases. What was clearly shown by these screening experiments is the possibility to stabilize IPC-1P layers with more expanded interlayer distances compared

to IPC-2 zeolite. In addition, some other alkoxysilylation agents were tested for the stabilization. The other molecules (1,3-diethoxy-1,1,3,3-tetramethyldisiloxane and 1,3,5,7,9,11,14-heptaisobutyltricyclo[7.3.3.15,11]heptasiloxane-endo-3,7,14-triol) were bigger than standard agent (DEDMS). The results did not vary much from the previous attempts and produced IPC-2 zeolite. Nevertheless, there is a possibility that other linkers especially with more atoms in the structure can be intercalated in between layers to produce new structures. Keeping in mind that intercalation chemistry allows to obtain the precursor with different interlayer distance, in principle the extension of stabilization could be likely. Perhaps it is possible to choose the intercalating agent (with desired size) and then apply the alkoxylating agent (with corresponding size) to produce the structure expanded beyond IPC-2 zeolite or even reassembly the **UTL** topology with silica D4R.

Second type of props introduced into the IPC-1P was organic ones. This resulted in the creation of inorganic-organic hybrids. Organic molecules containing silicon atoms were inserted into the IPC-1P(C_{16}TMA). The props were covalently bonded to the layers of zeolite via the condensation of terminal alkoxide groups with terminal Si-OH groups of IPC-1P. This produces porous materials that can be referred to as pillared with organic. These covalently bonded organic-inorganic materials combine the advantages of both components. Mechanical and structural stability of inorganic part, are complemented by high flexibility and possibility for functionalization of the organic props. The overall thermal stability is decreased due to the presence of organics, moreover stability of this part is limiting factor. Despite the limitations of such materials they can find the application under relatively mild conditions. The similar idea was executed for **MWW** layered zeolite [57]. That study accomplished the bridging of MCM-22P with silsesquioxanes as pillars. It shows a functionalization of benzene rings in the organic part of the hybrid with basic amino groups resulting in bifunctional acid-base catalysts. Based on this concept the experiments with IPC-1P were performed. Due to relatively large size of the molecules the intercalation of silsesquioxanes was executed using the swollen precursor. Organic-inorganic hierarchical hybrids with tailored textural properties can be produced from IPC-1P swollen with C_{16}TMA surfactant. Bridged silsesquioxanes (BSSs) and polyhedral oligomeric siloxane (POS) were introduced into swollen IPC-1SW after two days of stirring at 60 ^{o}C. Afterwards, the swelling agent was

removed by consecutive extraction using NH_4NO_3 and HCl solutions. In the final pillared material the intercalated molecules are covalently bonded with 2D zeolite layers.

Samples were described based on XRD [Fig. 4.1.12.], TEM, thermogravimetry and micropore size distribution analysis. The intercalate BSSs molecules used for modifications were 1,4-bis-(triethoxysilyl)benzene (BSS1), 1,2-bis-(triethoxysilyl)ethane (BSS2) and 4,4-bis-(triethoxysilyl)-1,1'-biphenyl (BSS3). Inorganic props were introduced by intercalation of octakis(tetramethylammonium)T8-siloxane (POS1). According to the interlayer distance in the final product it assumed that more than one linker molecule is connecting the layers. This system has mesopores or hierarchical micro-mesoporous systems exhibiting BET areas higher than 1000 m^2, micropore volumes above 0.3 cm^3/g and total pore volumes over 1 cm^3/g. Thermal stability of these hybrid materials is up to 350 ^oC which can be described as relatively high for such kind materials. Textural properties of this type or layered materials with organic pillars can be varied. Desired properties can be obtained by the manipulation with the ratio between layered precursor and organic species forming pillars.

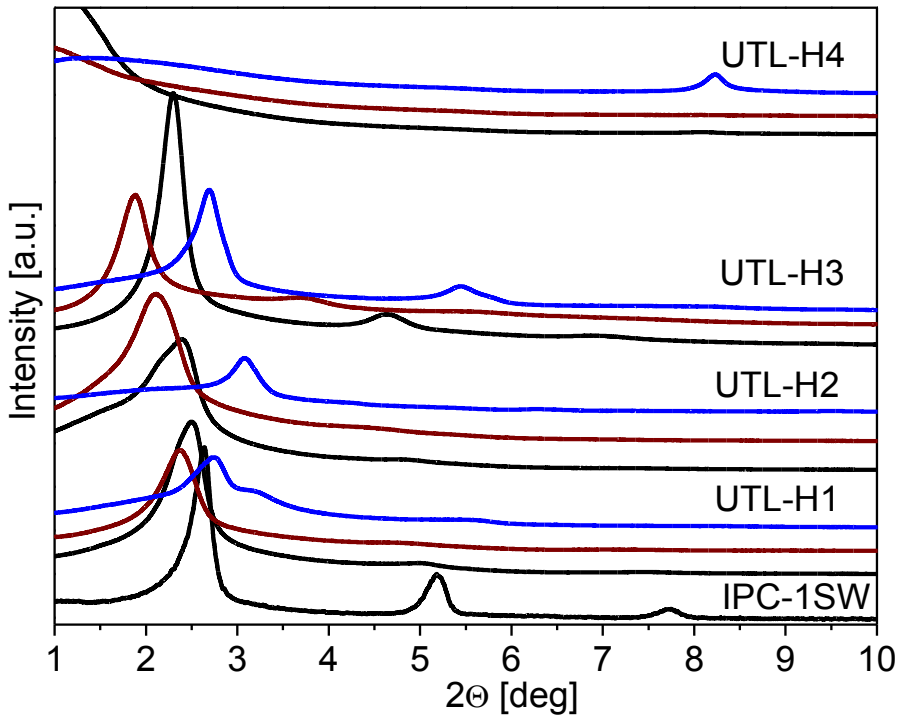

Fig. 4.1.12. XRD patterns of the IPC-1SW (at the bottom) and synthesized hybrid materials with different intercalating agent/IPC-1SW w/w ratio: 1 – black, 1.5 – red, 2 – blue.

4.2. Layer manipulation – shift of the layers

The particularly challenging goal of the thesis was exploration of interlamellar chemistry of IPC-1P, especially focused on the finding of a synthetic pathway to get the predicted “unfeasible” zeolite structures. On one hand, this challenge was considered as achievable according to the hypothetical deliberations on the arrangement of surface silanols of layered precursor. On the other, this task was demanding, as the lateral shift of layers followed by their reassembly in the shifted ordering was not preferred from the energy point of view. ADOR strategy of zeolite synthesis is essentially different from the traditional methods. This difference was a key to get the “unfeasible” zeolites, which structures are discussed below.

The synthesis of IPC-4 showed that it is possible to organize the IPC-1P layers and reassembly them towards new zeolite structure by calcination. If this reassembly was preceded by intercalation of additional alkoxysiloxane the product is another zeolite IPC-2. In both cases, the orientation of layers with respect to each other is the same as in the parent **UTL** zeolite. Reconnection of IPC-1P layers in that way does not require the lateral shift. Produced zeolites, IPC-4 and IPC-2, obey all LID criteria [41] and are described as feasible, even towards solvothermal synthesis. Reconnections through oxygen bridges or S4Rs do not introduce any strain into new materials. To produce 'unfeasible' zeolites it was predicted that the relative arrangement of the layers needs to be changed to introduce a geometric mismatch between them. This is exploited by the controllable lateral shift of the layers with respect to each other and consecutively by reassembly of them in that configuration by forming oxygen bridges or S4Rs. The shifted structures have been predicted [74] as hypothetical zeolites possible to prepare due to the special distribution of the silanols in IPC-1P. Layered precursor has relatively high concentration of surface silanols (1 silanol/ 43 $Å^2$) located as quadruplets [Fig. 2.7].

DFT calculations showed that there are four possible arrangements of reconnected IPC-1P layers. As outcome, four new defined structures were proposed. One of the predicted structures, prepared without lateral shift, was IPC-4 (**PCR**) zeolite [Fig. 4.2.1.a].

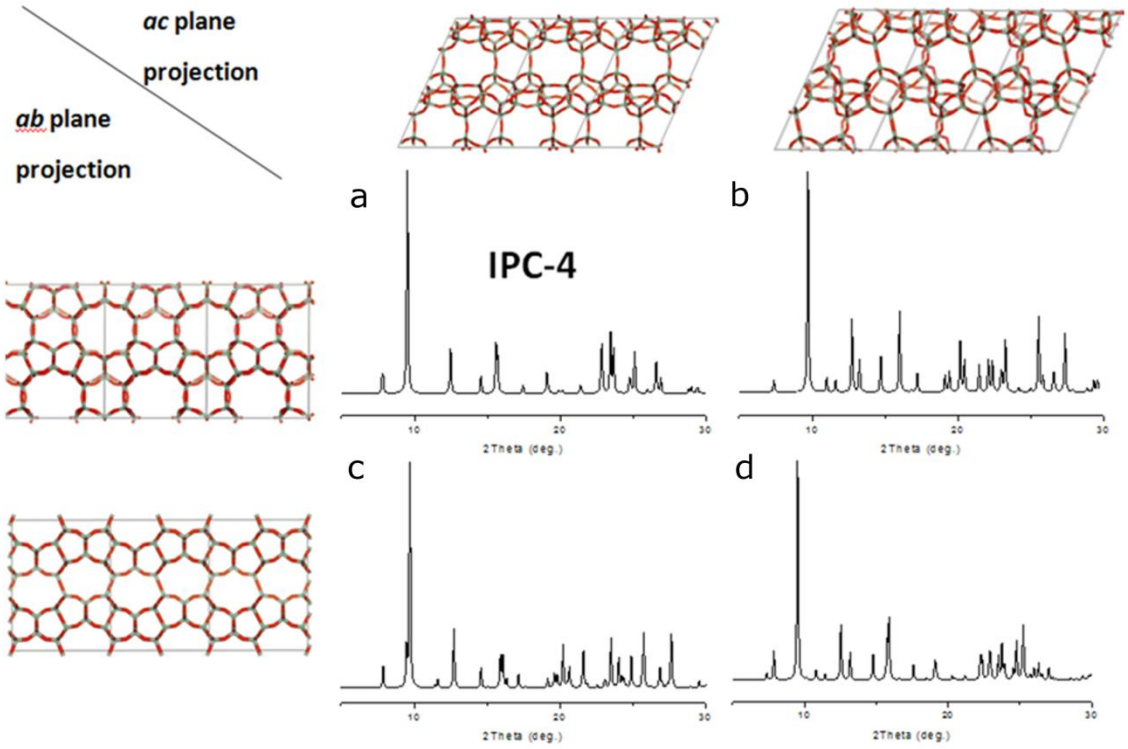

Fig. 4.2.1. Four predicted structures possible to obtain by reassembly of IPC-1P layers by connection with oxygen bridges.

Topological analysis shows that all four possible structures are unique. Unlike **PCR**, three other architectures require a lateral shift of layers, though each of it in different crystallographic direction(s). Consequently, all four structures have particular channel system. Directly connected IPC-4 (**PCR**) has intersecting 10-ring and 8-ring channels [Fig. 4.2.1.a.]. Shifting the layers along *b* vector results in the reduction of the channel running along *c* from 10-ring to 8-ring while size of 8-ring channel along *b* axis is unaffected. In other words, the structure shifted towards *b* axis has intersecting 8-ring and 8-ring channels [Fig. 4.2.1.c.]. The shift of layers along *c* axis leads to reduction of 8-ring along *b* to 7-ring. Resulting material has 10-ring x 7-ring intersecting channels [Fig. 4.2.1.b.]. Finally, the last possibility is the shift along both *b* and *c* axis, as a result the channel system of this topology is intersecting 8-ring x 7-ring [Fig. 4.2.1.d.]. Some of those possible arrangements produce zeolites with odd-ring channel systems, which is very rare in case of known zeolites prepared by standard methods. Significant differences between those 4 topologies are observable in simulated PXRD patterns [Fig. 4.2.2.]. Structural parameters of those architectures are summarized in Table

4.2.1. Relative energy of **PCR** framework is 0 kJ·mol^{-1} [74]. Relative energies of the frameworks shifted only in one direction are 105 and 109 kJ·mol^{-1} for shift along *c* and *b* vectors, respectively. The difference in relative energy between those two is relatively small indicating that they should be evenly like to prepare, in principle. The highest framework energy (186 kJ·mol^{-1}) corresponds to layers shifted along both *b* and *c* vectors [74]. This is expected because this shift is the most demanding and causes the biggest strain in the structure among those four. It suggests that this shift is less probable to get synthetically. According to the calculations, zeolites shifted along *c* axis break at least one of LID criteria, while the one shifted along *b* satisfies all of them.

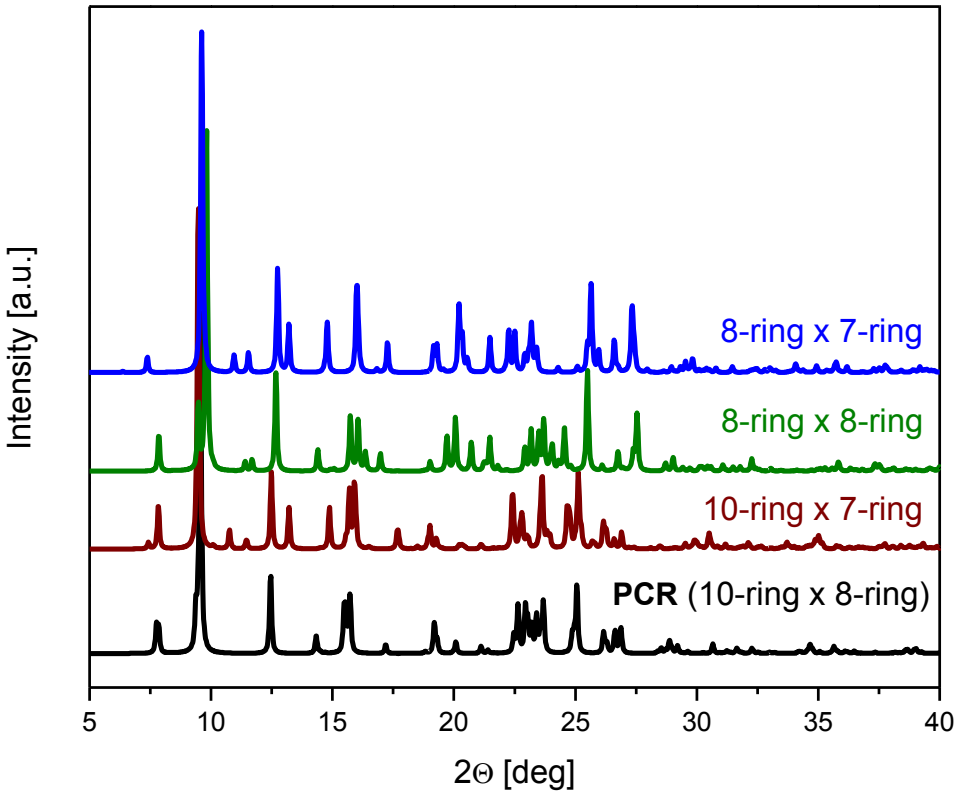

Fig. 4.2.2. Theoretical XRD patterns of four possible architectures to gain after reassembly of IPC-1P layers with oxygen bridges between them.

Table 4.2.1. Structural parameters of four possible architectures to gain after reassembly of IPC-1P layers with oxygen bridges between them.

Channel system	a [Å]	b [Å]	c [Å]	α [°]	β [°]	γ [°]	Space group
10-ring x 8-ring (**PCR**)	20.462	14.200	12.615	90.00	115.42	90.00	C 2/m
10-ring x 7-ring	15.544	14.168	12.168	89.69	131.12	117.31	P 1
8-ring x 8-ring	10.038	13.960	12.116	90.00	111.74	90.00	P m
8-ring x 7-ring	9.363	13.881	12.199	90.00	101.03	90.00	P m

Even more complicated is the case of the lateral shift of the layers with simultaneous reconnection of them by S4R building units. Totally 16 different structures were suggested for this kind of reassembly [99]. However, the topological analysis revealed that only 8 of them are unique. One of the possibilities is IPC-2 (zeolite with **OKO** topology). This is the only alteration among them, which satisfies the LID criteria [99]. All other possible structures containing S4R species as connecting unit have higher framework energy, thus their feasibility factors are larger [99].

The energetics calculated for the 'shifted' structures (3 alterations for layers with oxide bridges, and 7 alterations for layers with S4Rs in between) placed them in the group of 'unfeasible' zeolites. This conclusion has been made based on the LID criteria and location of this zeolite above the energy-density line [41], which were defined for zeolites obtained by solvothermal method. The question was if the uniqueness of ADOR approach, so different from standard synthesis, would be suitable to get at least some of those predicted zeolites. And the answer was affirmative. ADOR strategy is useful for the synthesis of zeolites previously concerned as unfeasible targets. It was proved by development of the experimental pathway to get two new zeolites: IPC-9 and IPC-10, shifted alterations of **PCR** and **OKO** topologies, respectively.

4.2.1. New ‘unfeasible’ zeolite prepared by direct condensation: IPC-9

Synthesis of IPC-9 was possible by the control of the layers organization. The layers of IPC-1P have to be shifted in respect to each other towards *c* crystallographic axis. To achieve this it was necessary to fulfil two requirements. First one is to break the hydrogen bonding between the layers. The separation of layers was discussed in

chapter 4.1.1. In basic pH (pH approximately 13) the surface silanols are deprotonated, and hydrogen bonds are broken. This allows the layers to change the original alignment. Next important issue is the organization of layers with designed alignment. Both of these two conditions have to be satisfied.

The synthesis was realized in two different ways. One is a two-step method, in which large surfactant molecules (C_{16}TMA-OH) are at first intercalated in between layers, and at second, de-intercalated in the presence of SDA (choline) molecules that favours the desired relative arrangement of the layers. Alternatively, one-step method can be performed using the basic conditions (pH ≈ 13) to deprotonate the silanol groups on the layer surface and, simultaneously intercalate proper SDA (choline or DEDMA) in hydroxide form into the structure. Then, SDA was intercalated into IPC-1P forming shifted precursor IPC-9P. To produce IPC-9 zeolite, shifted precursor was calcined at 550 ^{o}C for 8h with a ramp of 1 ^{o}C/min. During calcination step the layers were connected by condensation of silanols. SEM image shows that the crystals of obtained zeolite are smaller than original IPC-1P [Fig. 4.2.7.]. The partial dissolution of crystals is probably due to the intercalation at relatively high pH.

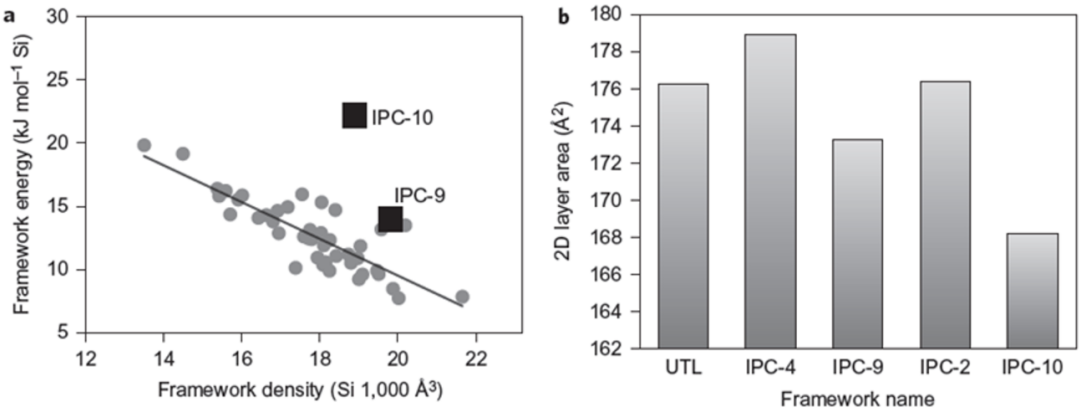

Fig. 4.2.3. The energetics of IPC-9 and IPC-10 (a) The positions of IPC-9 and IPC-10 in energy-density space (squares) in comparison to the positions of all other known silica zeolites (circles). Typical energy-density correlation is marked as black line. (b) Comparison of the 2D unit-cell area parallel to the UTL-like layers demonstrating contraction of layers in IPC-9 and IPC-10 in comparison to their feasible analogues (IPC-4 and IPC-2 respectively).

The IPC-9 zeolite has 10-ring x 7-ring channel system. It means the layers are shifted along *c* axis compared to non-shifted IPC-4 alignment. The shift is of half unit cell long. Choline cation as SDA is suitable for this shift. This organic molecule favours the desired, shifted orientation of the layers. Density functional theory (DFT) studies on the interactions between choline cations and surface silanols quadruplets predict that cation will preferentially locate between them. Studies also indicated that the most-favorable arrangement of multiple layers presumably depends on the amount of choline intercalated in the interlayer space. At low choline concentrations (choline to silanol ratio = 1 : 4) the layers would be shifted from their original IPC-1P position towards crystallographic *b* direction. In contrast, when the choline amount is higher (choline to silanol ratio = 1:2), the most favorable shift is, like in the IPC-9, towards *c* axis. The experiments showed good agreement with the calculations. The XRD pattern of the precursor intercalated with choline (denoted IPC-9P) is consistent with that predicted for the *c*-shifted material with high choline content. The refinement of the final, calcined IPC-9 structure also showed great agreement with the predicted, simulated pattern. Structure of IPC-9 was confirmed by comparison the experimental pattern to the simulated one by whole-pattern (Le Bail type) refinement of the unit cell against the X-ray diffraction data. Further, structure was also refined by Rietveld refinement of the structural model against the XRD data [Fig. 4.2.4.]. Moreover, the HRTEM technique allowed to confirm the structure by comparison with the model [Fig. 4.2.6.].

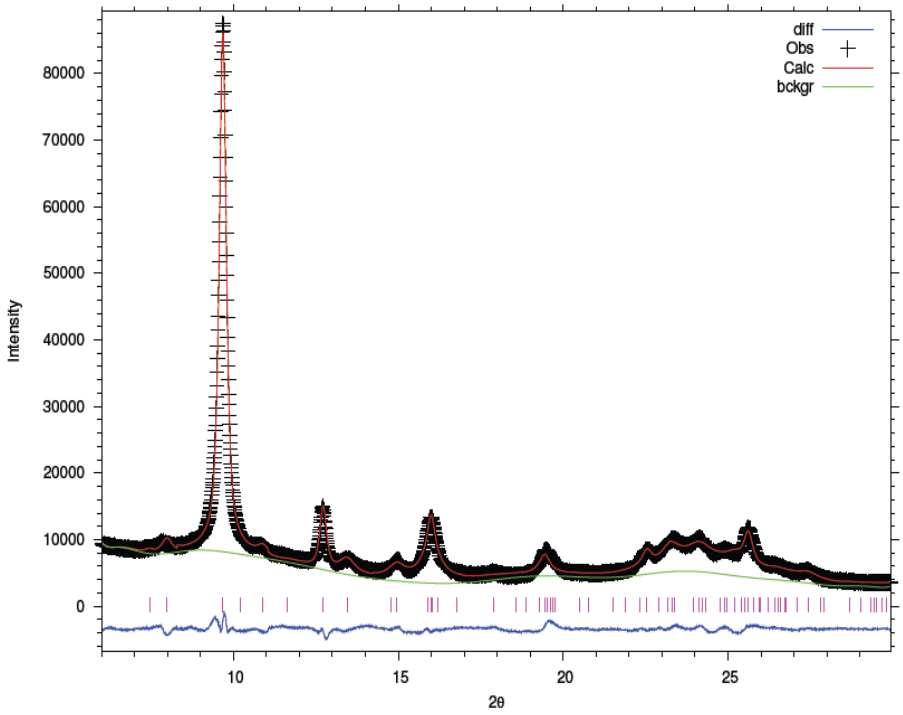

Fig. 4.2.4. Rietveld refinement of IPC-9 structure.

Table 4.2.1. Crystallographic data from the Rietveld refinement of IPC-9 zeolite.

a	18.6695(20) Å
b	13.8984(15) Å
c	12.1020(30) Å
β	102.409(34) °
Space group	C 2/m
Geometric Restraints	
Si-O	1.61(2)
O-O	2.62(3)
Si-Si	3.07(4)
R_{F2}	0.0296
wRp	0.0315
Rp	0.0260

Very interesting feature of the IPC-9 framework is odd-number channel (7-ring) [Fig. 4.2.5.]. It is relatively rare feature in case of zeolites. Up to date, known zeolite structures have only very few seven-rings [45]. All known zeolites can be found at the low-density edge of the energy-density distribution [Fig. 2.1.]. Predicted structures with low density have relatively few seven-rings and odd-rings in general. Apparently,

the constraint of proximity to the low-density edge of predicted structures leads to a low probability of 7-rings in zeolites [45].

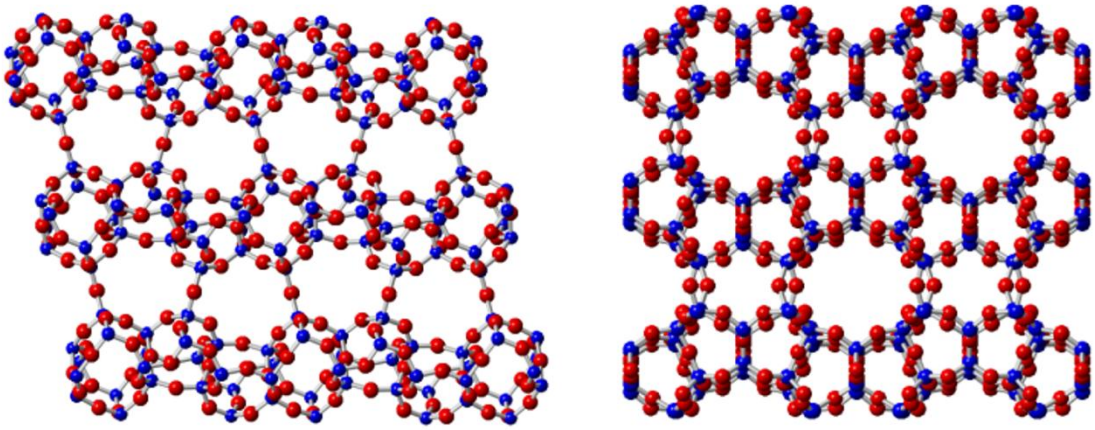

Fig. 4.2.5. The structure of IPC-9 viewed parallel to the 7-ring channels (010) in the structure (left) and parallel to the 10-ring channels (001) (right).

It is necessary to underline that the IPC-9 is fully four-connected, well crystalline zeolite [Fig. 4.2.5.] without remaining internal free silanol groups. Moreover, this structure has interesting energetics and was concerned as theoretically ‘unfeasible’ synthetic target [Fig. 4.2.3.]. That will be discussed in details in unit 4.3.

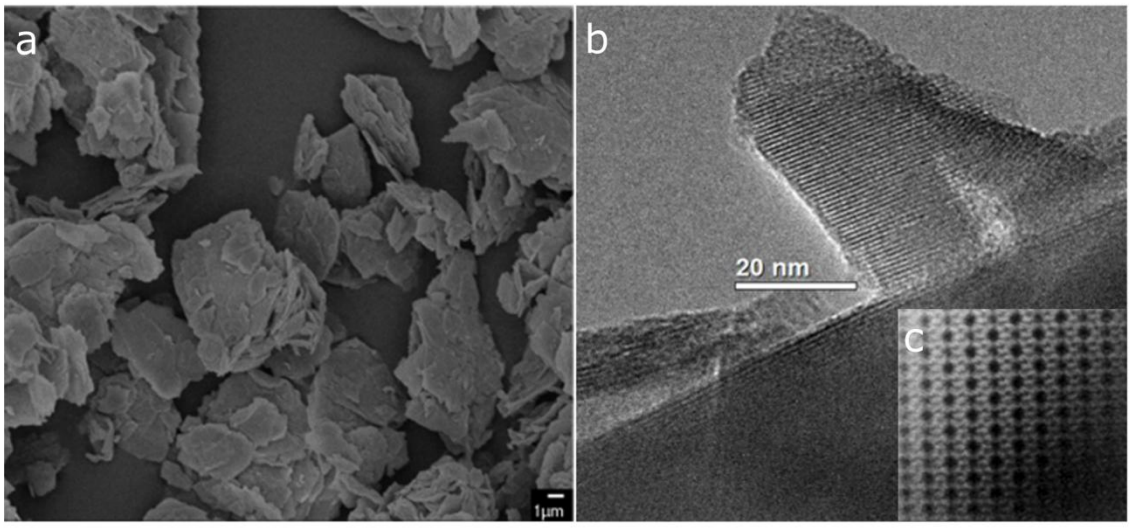

Fig. 4.2.6. SEM (a) and HRTEM (b,c) images of IPC-9 ‘unfeasible’ zeolite.

4.2.2. New ‘unfeasible’ zeolite prepared by alkoxysilylation: IPC-10

Next newly synthesized zeolite, denoted as IPC-10, has been also prepared starting with the shift of layers. The IPC-9 was prepared by calcination with zeolite precursor intercalated with choline cations - IPC-9P. In the case of IPC-10, the additional silicon atoms were added (in the form of DEDMS) and intercalated between the layers. This process is analogical to the synthesis of IPC-2 zeolite, with the difference in the initial arrangement of precursor layers. IPC-9P after alkoxysilylation, followed by calcination, produces a shifted structure with added S4R units connecting layers. IPC-10 is fully connected zeolite without any remaining silanols which was confirmed by MAS NMR. The SEM image shows that, like in case in IPC-9, the crystals are smaller than initial IPC-1P [Fig. 4.2.7.]. This is caused by treatment at high pH (pH = 13) during intercalation of choline. IPC-10 has the same layer arrangement as IPC-9 (shifted by half unit cell towards crystallographic c direction). The creation of single-four ring units leads to slightly more complex structural arrangement because there are two possible ways, in which the S4Rs can be formed with the same layer arrangement. Theoretical calculations (DFT) indicate that those two possibilities are very close to each other in term of energy (the difference between them is only 2 kJ mol^{-1} per silicon). This suggests that both forms may be simultaneously present in the material, which leads to some disorder in the interlayer region. The disordered nature of IPC-10 was confirmed by HRTEM [Fig. 4.2.7.] The channel system in this zeolite comprises 12-ring x 9-ring, regardless of the way of formation of S4Rs [Fig. 4.2.8.]. The structure was identified by comparison of the experimental X-ray diffraction pattern with that predicted from computational studies using Le Bail fit [Fig. 4.2.9.] and [Table 4.2.2.].

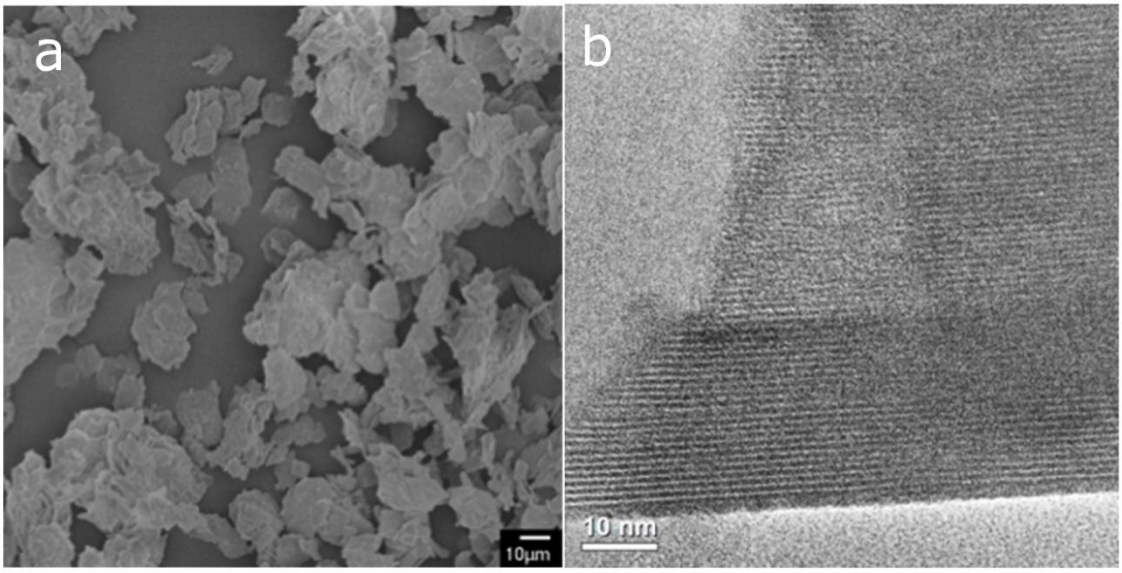

Fig. 4.2.7. SEM (a) and HRTEM (b) images of IPC-10 'unfeasible' zeolite.

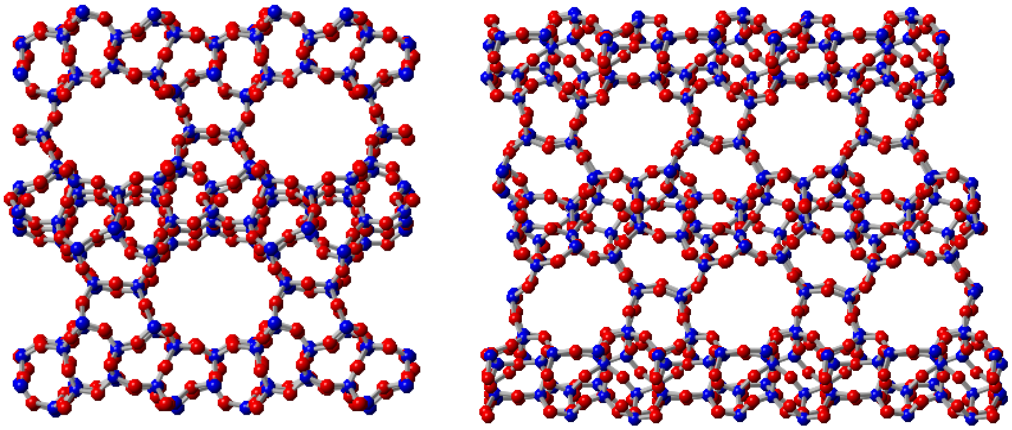

Fig. 4.2.8. The structure of idealized IPC-10 viewed parallel to the 9-ring channels (010) (left), and parallel to the 12-rings (001) (right).

Table 4.2.2. Crystallographic data from the Le Bail refinement of IPC-10 zeolite.

a	22.261(2) Å
b	13.852(2) Å
c	11.809(6) Å
α	87.22(5) ^{o}
β	97.78(3) ^{o}
γ	91.90(2) ^{o}
Space group	P-1
wRp	0.0287
Rp	0.0166

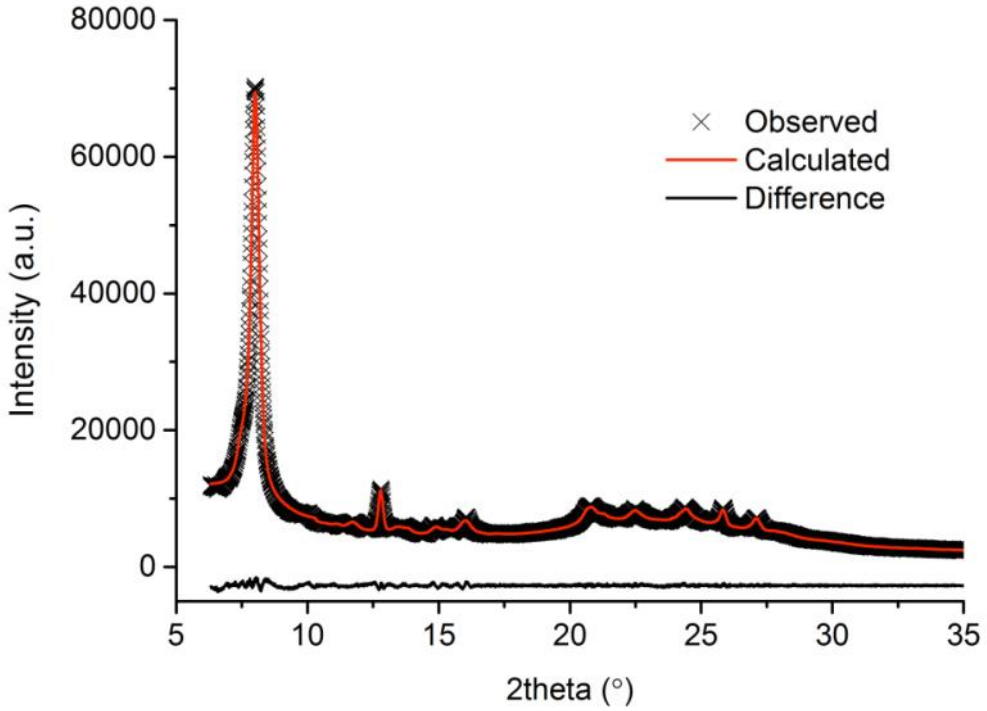

Fig. 4.2.9. The Le Bail fit for the IPC-10 structure.

IPC-10, similarly to IPC-9, has odd-number channels in the structure (9-ring channels). 9-rings are even less probable than 7-rings to appear in zeolite structure [45]. Also the energetics of IPC-10 is unprecedented, so this new zeolite, as well as IPC-9, would be considered as unfeasible synthesis target in the case of standard, solvothermal synthesis [Fig. 4.2.3.].

4.3. New insights into zeolite feasibility

There have been several attempts to rationalize the feasibility of zeolites as synthesis targets. This results in the proposal of feasibility factor, ϑ, which should be as near zero as possible. This factor can be calculated based on Sanders-Leslie-Catlow (SLC) force field method. Essentially, it is a measure how close the framework energy of the material lies to the ideal energy-density correlation [105]. Calculation shows that feasibility factor for IPC-9 is 1.7, while for IPC-10 is 4.9 which is relatively huge number.

Also the Local Interatomic Distance (LID) criteria were developed as a way to describe the feasibility of framework synthesis. LID criteria describe the local distortions from idealized tetrahedron that are possible in feasible zeolites. There are five criteria, and all of them are met by all previously known zeolite materials. The average distances between atoms ($<D_{TO}>$, $<D_{OO}>$ and $<D_{TT}>$) were collected in Table 4.3.1.

Table 4.3.1. Average T-O, O-O, and T-T distances (<D>), standard deviation values for average distances (σ), the values that the distances adopt from average (R), and the measures of the distortions (ε).

	PCR	**OKO**	IPC-9	IPC-10
$<D_{TO}>$	1.5981	1.6022	1.6012	1.6054
σ_{TO}	0.0061	0.0080	0.0095	0.0134
R_{TO}	0.0268	0.0406	0.0567	0.0687
$<D_{OO}>$	2.6093	2.6156	2.6134	2.6199
ε_{OO}	0.0002	0.0006	0.0010	0.0015
σ_{OO}	0.0333	0.0412	0.0495	0.0636
R_{OO}	0.1688	0.2106	0.3089	0.3542
$<D_{TT}>$	3.0926	3.0728	3.0784	3.0583
ε_{TT}	0.0009	0.0003	0.0000	0.0007
σ_{TT}	0.0401	0.0590	0.0728	0.0801
R_{TT}	0.1539	0.2297	0.3134	0.3498

All values in Å

The first LID criterion suggests that the average tetrahedron should be very close to an idealized tetrahedron, by saying that the values of $<D_{TO}>$ and $<D_{OO}>$ should fit the correlation described by equation $<D_{OO}> = 1.6284x<D_{TO}> - 0.0071$. $\varepsilon_{<OO>}$ is a measure of the distance away from this correlation and for all previously known zeolites this value was less than 0.0009. In the case of both IPC-9 and IPC-10 this criterion is not met [Table 4.3.1]. This suggests that the average tetrahedron in both structures is far away from the idealized one.

The second LID criterion is similar to the first one, except that it is a correlation between $<D_{TO}>$ and $<D_{TT}>$ is tested. The equation is as follows: $<D_{TT}> = -4.8929x<D_{TO}> + 10.9128$, and the distance from this correlation ($\varepsilon_{<TT>}$) should be less than 0.0046. This says that the T-T distances and T-O-T angles are within normal parameters for zeolites. In this case, the criterion is met both by IPC-9 and IPC-10 structures [Table 4.3.1].

The third criterion considers the standard deviation values (σ_{TO}, σ_{OO}, σ_{TT}) for the average distances (<D_{TO}>, <D_{OO}>, <D_{TT}>) respectively. The criterion states that these standard deviations should be within tight limits, meaning that local distortion of the structures are kept to a minimum. Specifically, the values should obey the relations: $\sigma_{TO} < 0.0196$, $\sigma_{OO} < 0.0588$, and $\sigma_{TT} < 0.0889$. IPC-9 passes this one, but IPC-10 fails the test for σ_{OO} [Table 4.3.1], indicating that some angles in this material show a larger distortion than is expected for a feasible structure.

The fourth criterion deals with the ranges of values that the T-O, O-O and, T-T distances can adopt. Namely, the distances should lie within the following ranges: $R_{TO} < 0.0634$ Å, $R_{OO} < 0.2746$ Å, and $R_{TT} < 0.3332$ Å. Neither IPC-9 nor IPC-10 passes this test having R_{TO} = 0.0567 Å, R_{OO} = 0.3089 Å, and R_{TO} = 0.0687 Å, R_{OO} = 0.3542 Å respectively.

The fifth criterion is for conventional zeolites only. The criterion is based on T-O distance saying that this value should be in the range of: $1.5967 < D_{TO} < 1.6076$ Å. Both IPC-9 and IPC-10 structures obey this criterion [Table 4.3.1].

Table 4.3.2. The values of framework energies for framework densities (calculated using both DFT and SLC force field) for zeolites IPC-9 and IPC-10. Also listed are ϑ (the feasibility factors) and the LID criteria (1=pass, 0=fail). For comparison, data for zeolite with PCR and OKO topologies are listed.

Structure	Designation	FE_{DFT}[a]	FE_{FF}[a]	FD_{DFT}[b]	FD_{FF}[b]	ϑ	LID criteria				
							1	2	3	4	5
UTL-D4R(C2/m)	**PCR**	9.1	10.4	18.1	19.3	1.4	1	1	1	1	1
UTL-S4R(C2)	**OKO**	11.2	13.8	17.0	17.8	0.5	1	1	1	1	1
UTL-D4R(P1)	IPC-9	12.5	14.0	18.7	19.8	1.7	0	1	1	0	1
UTL-S4R(P-1)	IPC-10	16.8	20.1	18.0	18.8	4.9	0	1	0	0	1

[a] in $kJ \cdot mol^{-1}$, [b] in 10^{-3} $Å^{-3}$

The comparison of the feasibility factors and LID criteria is shown in Table 4.3.2. Shifted structures have significantly higher ϑ values than structures with original alignment. There are differences in the comparison of LID criteria agreement. **PCR** and **OKO**, both obey all 5 criteria while IPC-9 does not meet two of them, and IPC-10 disagrees in case of three of them. This is the reason why shifted structures were called 'unfeasible'. Also the framework energies of them show interesting outcome, especially in comparison to these values for all known zeolites. Figure 4.2.3a shows the energy-density plot for all known silica zeolites and demonstrates the location of IPC-9 and IPC-10 on it. IPC-9 lies

at the edge of the region in which known zeolites can be found. IPC-10 has even higher energy for its density because it lies well outside the region populated by known zeolites. In the case of IPC-10 it is very clear that it does not obey the standard correlation between framework energy and density (marked by red line). The slight geometric mismatch needed to form these two 'unfeasible' frameworks can be seen in a reduction of a product of a unit cell parameters b and c that corresponds to the interlayer directions. For IPC-9 the contraction is smaller (about 3.2 % compared to the IPC-4) than this value for IPC-10 (almost 5 % in comparison to IPC-2) [Fig. 4.2.3b].

All these calculations and comparison with previously known structures show that IPC-9 and IPC-10 materials would not be considered as feasible synthetic targets in the case of solvothermal synthesis. Among those two zeolites, IPC-10 meets less LID criteria and have higher feasibility factor. This brings the conclusion that the LID criteria should be re-considered, due to new synthetic outcomes. The ADOR strategy had shown the way to prepare materials that probably would not be possible to gain towards conventional, solvothermal route.

4.4. ADOR as universal strategy to create new materials

The most important outcome of the presented results is not the new zeolites themselves. The most important outcome is the discovery and extension of general method for synthesis of new zeolites – ADOR. The next meaningful is the fact, that the initially suggested criteria of feasibility can be overcome. There are at least two previously 'unfeasible' zeolites that are currently synthesizable materials. In principle ADOR is an excellent method to be applicable for other germanosilicates, which should be able to produce layered precursors. Presumably, the frameworks with similar architecture to **UTL** could be used in ADOR. Germanium has been found to preferentially occupy D4Rs. This feature was essential for the top-down synthesis of IPC-1P, as the very first step of ADOR applied for **UTL** zeolite. There are other germanosilicates with D4R units reported, but not every of them is expected to be ADOR applicable. There are some conditions that have to be met to consider zeolite as

'ADORactive'. Clearly, the first requirement is the presence of germanium in the framework and moreover, specific location of Ge in D4R (or in some cases in D3R) units. Also, the location of those units in the structure and their connectivity is important. There are two possible arrangements for such materials. The first can be considered as 1-dimensional location of D4Rs in the structure. The units appear only along one axis, so the structure of zeolite is based on the silica layers connected with germanium 'pillars'. Breaking of all interlayer bonds via hydrolysis would result in 2D lamellas like IPC-1P in case of **UTL**. This kind of architecture has been described for **ITH**, **IWW**, **ITR**, **UOV**, and some other topologies [99]. Second type of D4R location is in two dimensions. It means they are located not only in between layers, but some of them are part of layers in one direction. Hydrolysis of such type of architecture, for instance **IRN** or **UWY**, would probably cause the separation of the framework along 2 two axes. It may result in 1-dimensional zeolitic fibers or chains. Last possibility is location of D4R in framework in all 3 dimensions, i.e. for **BEC**, **IWS**, **IRR**, and **STW** zeolites [33]. It means that full hydrolysis of this kind of material would lead to the total fragmentation of the structure. The first group among three presented is consider as potentially usable is ADOR strategy. It means that at least 8 zeolites can be examined as probable parent materials for ADOR. Keeping in mind that **UTL** zeolite was exploited to create many new zeolites, including two previously considered as unfeasible, the in-depth study of other topologies can bring the whole class of new materials as the outcome.

It opens a huge number of potentially obtainable structures. This work proved that the conventional look on the feasibility of hypothetical zeolites can be expanded by new synthetic approach - ADOR. Zeolite conundrum is the fact that, even though there are millions of hypothetical structures calculated, only few of them have actually been prepared experimentally. The advances presented herein give hope that this conundrum is solved.

5. Conclusions

The interlamellar space of IPC-1P zeolite precursor was explored using different synthetic pathways. The IPC-1P is a layered material made by hydrolysis of **UTL** germanosilicate. Using various organic compounds the intercalation in between the IPC-1P layers was performed. Intercalation was a cause of expansion of the interlayer distance. The scale of expansion depends on the used agent. The separation of the layers requires relatively high pH, achieved by addition of tetrapropylammonium hydroxide solution or by ion-exchange of initial salt. The intercalation process was controlled and the features of produced material were designable. The IPC-1P layers were expanded with various distances and organized in different ways.

The intercalation was followed by reconnection of the layers by calcination. The product of the calcination of amine intercalated IPC-1P was mostly IPC-4 zeolite (**PCR**). The calcination of pure, non-intercalated precursor usually did not produce a highly ordered zeolite but disordered IPC-1 material. It was concluded that amines are able to organize the layers of precursor. Calcination of intercalated precursors with relatively large initial basal spacing showed that long interlayer distance makes the organization of layers and formation of ordered, well-defined structures more difficult.

Alkoxysilylation of the lamellar precursor showed that it is possible to stabilize the layers with distance longer than IPC-2 (**OKO**) structure. Those materials were thermally stable and presumably could lead to new architecture. More expanded structures are not fully described and should be further investigated.

The organized layered precursor was modified by introducing permanent props in between layers. The props were of different nature, inorganic amorphous silica pillars and organic silsesquioxanes. The final materials diversified due to the textural properties such as BET area, micropore and mesopores volumes. Inorganic pillaring showed that properties of those materials are designable in wide range. The introduction of organic parts showed the possibility of further functionalization of those materials. Although, the thermal stability of inorganic-organic hybrids was lower than pure inorganic pillared materials, still they were relatively stable and can be potentially use under milder conditions (up to 350 ^{o}C). This resulted in preparation of series of different materials using the same starting precursor.

The intercalation was used mainly as a part of investigated ADOR approach. This synthesis strategy led to two new, previously predicted, zeolites - IPC-9 and IPC-10 [Fig. 5.1]. These structures are exceptional because of their 'unfeasibility' in term of standard synthetic approach. Moreover, those new zeolites have rare structural features and can potentially be used e.g. as catalysts. The study has shown that ADOR strategy is suitable for the synthesis of materials that probably would not be possible to prepare by solvothermal method. The feasibility of zeolite synthesis was discussed in details showing that some rules and feasibility factors should be reconsidered. The rules which are obeyed by materials prepared in a standard way are not fully applicable on the zeolites prepared by novel ADOR approach.

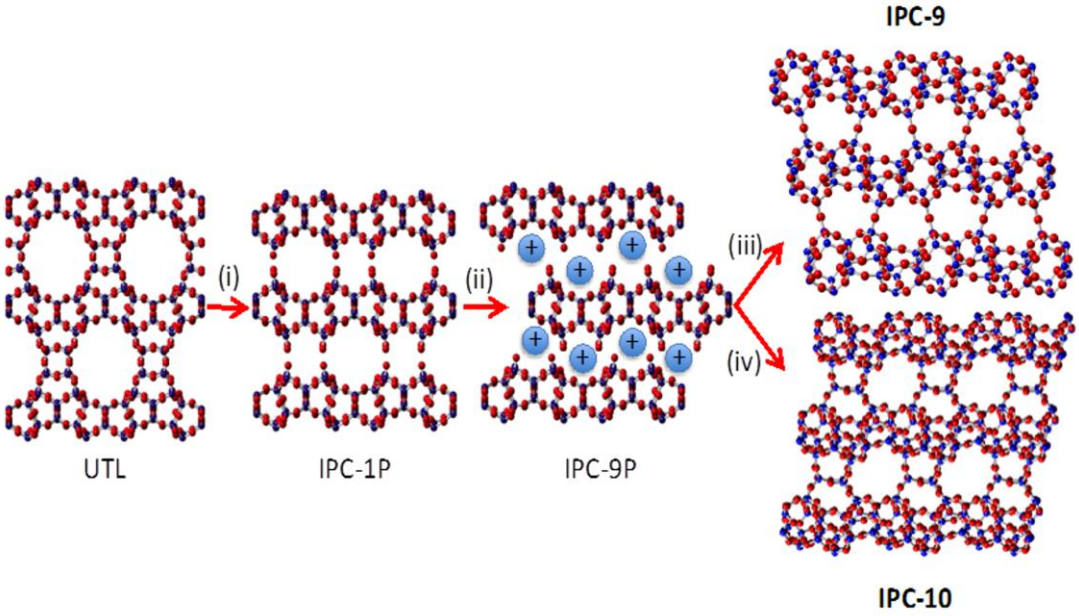

Fig. 5.1. The scheme showing synthetic pathway to obtain 'unfeasible' zeolites. (i) disassembly of **UTL** to IPC-1P zeolite precursor, (ii) shift of layers realized by intercalation of choline or DEDMA to get IPC-9P, (iii) direct condensation of IPC-9P to IPC-9 zeolite, (iv) alkoxysilylation of IPC-9P to IPC-10 zeolite.

The perspectives for further investigation of the interlamellar space of 2D zeolites are very vast. First of all, there are other germanosilicates that can be, in principle, "ADORactive". Extension of the ADOR process to other zeolites is the biggest challenge in the future. Secondly, it would be interesting to use the materials with tuneable properties for catalytic applications, e.g. after functionalization of them with heteroatoms. The precise control of the size of pores would be probably in designing of

the catalysts for bulky molecules transformations. However, the most promising outcome is related to the zeolite conundrum. The ADOR method is a pathway suitable for producing the materials probably out of reach for solvothermal synthesis, which indicates that in the long term the number of accessible zeolites will be increased vastly.

The study on the interlamellar space of two-dimensional zeolite precursor, IPC-1P, showed the big diversity in the products possible to prepare using it. Especially, the new synthetic strategy - ADOR - was proved to be exceptional way to prepare the materials unlike to get by conventional methods.

6. References

1. Introduction to zeolite science and practise; J. Čejka, H. van Bekkum, A. Corma, F. Schüth (Eds.); Studies in Surface Science and Catalysis, Vol. 168, third ed., Elsevier, Amsterdam, **2007**.
2. Cundy, C. S.; Cox, P. A., *Chem. Rev.* **2003,** *103*, 663-701.
3. Čejka, J.; Wichterlova, B., *Catal. Rev. Sci. Eng.* **2002,** *44*, 375-421.
4. Martinez, C.; Corma, A., *Coord. Chem. Rev.* **2011,** *255*, 1558-1580.
5. Moliner, M., *Dalton Trans.* **2014,** *43*, 4197-4208.
6. Primo, A.; Garcia, H., *Chem. Soc. Rev.* **2014,** *43*, 7548-7561.
7. Schwartz, T. J.; O'Neill, B. J.; Shanks, B. H.; Dumesic, J. A., *ACS Catal.* **2014,** *4*, 2060-2069.
8. Li, K.; Valla, J.; Garcia-Martinez, J., *ChemCatChem* **2014,** *6*, 46-66.
9. Fechete, I.; Wang, Y.; Védrine, J. C., *Catal. Tod.* **2012,** *189*, 2-27.
10. Gascon, J.; Kapteijn, F.; Zornoza, B.; Sebastian, V.; Casado, C.; Coronas, J., *Chem. Mater.* **2012,** *24*, 2829-2844.
11. Kosinov, N.; Auffret, C.; Sripathi, V. G. P.; Gucuyener, C.; Gascon, J.; Kapteijn, F.; Hensen, E. J. M., *Microporous Mesoporous Mater.* **2014,** *197*, 268-277.
12. Cheung, O.; Hedin, N., *RSC Adv.* **2014,** *4*, 14480-14494.
13. Mofarahi, M.; Gholipour, F., *Microporous Mesoporous Mater.* **2014,** *200*, 1-10.
14. Anderson, M.; Wang, H.; Lin, Y. S., *Rev. Chem. Eng.* **2012,** *28*, 101-121.
15. Breck, D. W., *J. Chem. Educ.* **1964,** *41*, 678-689.
16. Zeolite molecular sieves: structure, chemistry, and use; D.W. Breck; Wiley, New York, **1973**.
17. Davis, M. E., *Nature* **2002,** *417*, 813-821.
18. Barrer, R. M., *J. Chem. Soc.* **1948**, 127-132.
19. Atlas of Zeolite Framework Types, in: C. Baerlocher, L.B. McCusker, D.H. Olson, Elsevier, Amsterdam, 2007.
20. Cundy, C. S.; Cox, P. A., *Microporous Mesoporous Mater.* **2005,** *82*, 1-78.
21. Davis, M. E.; Lobo, R. F., *Chem. Mater.* **1992,** *4*, 756-768.

22. Schmidt, J. E.; Deem, M. W.; Davis, M. E., *Angew. Chem. Int. Ed.* **2014,** *126*, 8512-8514.
23. Gomez-Hortigueela, L.; Lopez-Arbeloa, F.; Cora, F.; Perez-Pariente, J., *J. Am. Chem. Soc.* **2008,** *130*, 13274-13284.
24. Jackowski, A.; Zones, S. I.; Hwang, S.-J.; Burton, A. W., *J. Am. Chem. Soc.* **2009,** *131*, 1092-1100.
25. Wang, Z.; Yu, J.; Xu, R., *Chem. Soc. Rev.* **2012,** *41*, 1729-1741.
26. J. Yu, R. X., *Acc. Chem. Res.* **2010,** *43*, 1195-1204.
27. Moliner, M.; Rey, F.; Corma, A., *Angew. Chem. Int. Ed.* **2013,** *52*, 13880-13889.
28. Roth, W. J.; Nachtigall, P.; Morris, R. E.; Čejka, J., *Chem. Rev.* **2014,** *114*, 4807-4837.
29. Diaz, U.; Corma, A., *Dalton Trans.* **2014,** *43*, 10292-10316.
30. Li, J.; J. Yu, R. X.; Xu, R., *Proc. R. Soc. A* **2012,** *468*, 1955-1967.
31. Park, M. B.; Cho, S. J.; Hong, S. B., *J. Am. Chem. Soc.* **2011,** *133*, 1917-1934.
32. Li, Y.; Yu, J., *Chem. Rev.* **2014,** *114*, 7268-7316.
33. International Zeolite Association. Structure Commission. http://www.iza-structure.org/ (accessed May 17, 2016)
34. Earl, D. J.; Deem, M. W., *Ind. Eng. Chem. Res.* **2006,** *45*, 5449-5454.
35. Akporiaye, D. E.; Price, G. D., *Zeolites* **1989**, 23-32.
36. Pophale, R.; Cheesman, P. A.; Deem, M. W., *Phys. Chem. Chem. Phys.* **2011,** *13*, 12407-12412.
37. Klinowski, J., *Curr. Opinion Solid State Mater. Sci.* **1998**, 79.
38. Blatov, V. A.; Ilyushin, G. D.; Prosepio, D. M., *Chem. Mater.* **2013,** *25*, 412-424.
39. Foster, M. D.; Simperler, A.; Bell, R. G.; Friedrichs, O. D.; Paz, F. A. A.; Klinowski, J., *Nature Mater.* **2004,** *3*, 234-238.
40. Sartbaeva, A.; Wells, S. A.; Treacy, M. M. J.; Thorpe, M. F., *Nature Mater.* **2006,** *5*, 962-965.
41. Li, Y.; Yu, J. H.; Xu, R. R., *Angew. Chem. Int. Ed.* **2013,** *52*, 1673-1677.
42. Akporiaye, D. E.; Price, G. D., *Zeolites* **1989,** *9*, 321-328.
43. Henson, N. J.; Cheetham, A. K.; Gale, J. D., *Chem. Mater.* **1996,** *8*, 664-670.
44. Henson, N. J.; Cheetham, A. K.; Gale, J. D., *Chem. Mater.* **1994,** *6*, 1647-1650.
45. Li, X.; Deem, M. W., *J. Phys. Chem. C* **2014,** *118*, 15835-15839.

46. Morris, R. E.; Čejka, J., *Nature Chem.* **2015,** *7*, 381-388.
47. Morris, R. E.; James, S. L., *Angew. Chem. Int. Ed.* **2013,** *52*, 2163-2165.
48. Ramos, F. S. O.; Pietre, M. K. d.; Pastore, H. O., *RSC Adv.* **2013,** *3*, 2084-2111.
49. Roth, W. J.; Čejka, J., *Catal. Sci. Technol.* **2011,** *1*, 43-53.
50. Selvam, T.; Inayat, A.; Schwieger, W., *Dalton Trans.* **2014,** *43*, 10365-10387.
51. Roth, W. J.; Gil, B.; Marszalek, B., *Catal. Tod.* **2014,** *227*, 9-14.
52. Wu, P.; Ruan, J. F.; Wang, L. L.; Wu, L. L.; Wang, Y.; Liu, Y. M.; Fan, W. B.; He, M. Y.; Terasaki, O.; Tatsumi, T., *J. Am. Chem. Soc.* **2008,** *130*, 8178-8187.
53. Roth, W. J.; Čejka, J.; Millini, R.; Montanari, E.; Gil, B.; Kubu, M., *Chem. Mater.* **2015,** *27*, 4620−4629.
54. Roth, W. J.; Kresge, C. T.; Vartuli, J. C.; Leonowicz, M. E.; Fung, A. S.; McCullen, S. B., *Stud. Surf. Sci. Catal.* **1995,** *94*, 301-8.
55. Lawton, S. L.; Fung, A. S.; Kennedy, G. J.; Alemany, L. B.; Chang, C. D.; Hatzikos, G. H.; Lissy, D. N.; Rubin, M. K.; Timken, H.-K. C.; Steuernagel, S.; Woessner, D. E., *J. Phys. Chem.* **1996,** *100*, 3788-3798.
56. Leonowicz, M. E.; Lawton, J. A.; Lawton, S. L.; Rubin, M. K., *Science* **1994,** *264*, 1910-1913.
57. Corma, A.; Díaz, U.; García, T.; Sastre, G.; Velty, A., *J. Am. Chem. Soc.* **2010,** *132*, 15011-15021.
58. Roth, W. J.; Dorset, D. L., *Microporous Mesoporous Mater.* **2011,** *142*, 32-36.
59. Wheatley, P. S.; Morris, R. E., *J. Mater. Chem.* **2006,** *16*, 1035-1037.
60. Asakura, Y.; Takayama, R.; Shibue, T.; Kuroda, K., *Chem. Eur. J.* **2014,** *20*, 1893-1900.
61. Rojas, A.; Camblor, M. A., *Chem. Mater.* **2014,** *26*, 1161-1169.
62. Wang, Y. X.; Gies, H.; Lin, J. H., *Chem. Mater.* **2007,** *19*, 4181-4188.
63. Marler, B.; Stroter, N.; Gies, H., *Microporous Mesoporous Mater.* **2005,** *83*, 201-211.
64. Moteki, T.; Chaikittisilp, W.; Shimojima, A.; Okubo, T., *J. Am. Chem. Soc.* **2008,** *130*, 15780.
65. Roth, W. J.; Dorset, D. L., *J. Struct. Chem.* **2010,** *21*, 385-390.
66. Zanardi, S.; Alberti, A.; Cruciani, G.; Corma, A.; Fornes, V.; Brunelli, M., *Angew. Chem. Int. Ed.* **2004,** *43*, 4933-4937.

67. Ikeda, T.; Akiyama, Y.; Oumi, Y.; Kawai, A.; Mizukami, F., *Angew. Chem. Int. Ed.* **2004,** *43*, 4892-4896.

68. Yang, B.; Jiang, J.-g.; Xu, H.; Liu, Y.; Peng, H.; Wu, P., *Appl. Catal., A* **2013,** *455*, 107-113.

69. Park, W.; Yu, D.; Na, K.; Jelfs, K. E.; Slater, B.; Sakamoto, Y.; Ryoo, R., *Chem. Mater.* **2011,** *23*, 5131-5137.

70. Jung, J.; Jo, C.; Cho, K.; Ryoo, R., *J. Mater. Chem.* **2012,** *22*, 4637-4640.

71. Li, J.; Corma, A.; Yu, J., *Chem. Soc. Rev.* **2015,** *44*, 7112-7127.

72. Marler, B.; Wang, Y.; Song, J.; Gies, H., *Dalton Trans.* **2014,** *43*, 10396-10416.

73. Jordá, J. L.; Rey, F.; Sastre, G.; Valencia, S.; Palomino, M.; Corma, A.; Segura, A.; Errandonea, D.; Lacomba, R.; Manjón, F. J.; Gomis, Ó.; Kleppe, A. K.; Jephcoat, A. P.; Amboage, M.; Rodríguez-Velamazán, J. A., *Angew. Chem. Int. Ed.* **2013,** *52*, 10458-10462.

74. Roth, W. J.; Nachtigall, P.; Morris, R. E.; Wheatley, P. S.; Seymour, V. R.; Ashbrook, S. E.; Chlubná, P.; Grajciar, L.; Položij, M.; Zukal, A.; Shvets, O.; Čejka, J., *Nature Chem.* **2013,** *5*, 628-633.

75. Roth, W. J.; Shvets, O. V.; Shamzhy, M.; Chlubná, P.; Kubů, M.; Nachtigall, P.; Čejka, J., *J. Am. Chem. Soc.* **2011,** *133*, 6130-6133.

76. Paillaud, J. L.; Harbuzaru, B.; Patarin, J.; Bats, N., *Science* **2004,** *304*, 990-992.

77. Corma, A.; Diaz-Cabanas, M. J.; Rey, F.; Nicolooulas, S.; Boulahya, K., *Chem. Com.* **2004**, 1356-1357.

78. Shvets, O. V.; Kasian, N.; Zukal, A.; Pinkas, J.; Čejka, J., *Chem. Mater.* **2010,** *22*, 3482-3495.

79. Shvets, O. V.; Shamzhy, M. V.; Yaremov, P. S.; Musilová, Z.; Procházková, D.; Čejka, J., *Chem. Mater.* **2011,** *23*, 2573-2585.

80. Shamzhy, M. V.; Shvets, O. V.; Opanasenko, M. V.; Yaremov, P. S.; Sarkisyan, L. G.; Chlubná, P.; Zukal, A.; Marthala, V. R.; Hartmann, M.; Cejka, J., *J. Mater. Chem.* **2012,** *22*, 15793-15803.

81. Shvets, O. V.; Zukal, A.; Kasian, N.; Žilková, N.; Čejka, J., *Chem. Eur. J.* **2008,** *14*, 10134-10140.

82. Blasco, T., *J. Phys. Chem. B* **2002,** *106*, 2634-2642.

83. Corma, A.; Diaz-Cabanas, M. J.; Martinez-Triguero, J.; Rey, F.; Rius, J., *Nature* **2002,** *418*, 514-517.

84. Pulido, A.; Sastre, G.; Corma, A., *ChemPhysChem* **2006,** *7*, 1092-1099.

85. Sastre, G.; Pulido, A.; Corma, A., *Microporous Mesoporous Mater.* **2005,** *82*, 159-163.

86. Kasian, N.; Tuel, A.; Verheyen, E.; Kirschhock, C. E. A.; Taulelle, F.; Martens, J. A., *Chem. Mater.* **2014,** *26*, 5556-5565.

87. Zilkova, N.; Shamzhy, M.; Shvets, O.; Čejka, J., *Catal. Today* **2013,** *204*, 22-29.

88. Shamzhy, M. V.; Shvets, O. V.; Opanasenko, M. V.; Kurfiřtová, L.; Kubička, D.; Čejka, J., *ChemCatChem* **2013,** *5*, 1891-1898.

89. Xu, H.; Jiang, J.; Yang, B.; Wu, H.; Wu, P., *Catal. Commun.* **2014,** *55*, 83-86.

90. Kasian, N.; Vanbutsele, G.; Houthoofd, K.; Koranyi, T. I.; Martens, J. A.; Kirschhock, C. E. A., *Catal. Sci. Tech.* **2011,** *1*, 246-254.

91. Li, Q.; Navrotsky, A.; Rey, F.; Corma, A., *Microporous Mesoporous Mater.* **2003,** *59*, 177-183.

92. Li, Q.; Navrotsky, A.; Rey, F.; Corma, A., *Microporous Mesoporous Mater.* **2004,** *74*, 87-92.

93. Thang, H. V.; Rubeš, M.; Bludský, O.; Nachtigall, P., *J. Phys. Chem. A* **2014,** *118*, 7526–7534.

94. Verheyen, E.; Joos, L.; Van Havenbergh, K.; Breynaert, E.; Kasian, N.; Gobechiya, E.; Houthoofd, K.; Martineau, C.; Hinterstein, M.; Taulelle, F.; Van Speybroeck, V.; Waroquier, M.; Bals, S.; Van Tendeloo, G.; Kirschhock, C. E. A.; Martens, J. A., *Nature Mater.* **2012,** *11*, 1059-1064.

95. Fan, W. B.; Wu, P.; Namba, S.; Tatsumi, T., *Angew. Chem. Int. Ed.* **2004,** *43*, 236-240.

96. Wheatley, P. S.; Chlubná-Eliášová, P.; Greer, H.; Zhou, W.; Seymour, V. R.; Dawson, D. M.; Ashbrook, S. E.; Pinar, A. B.; McCusker, L. B.; Opanasenko, M.; Čejka, J.; Morris, R. E., *Angew. Chem. Int. Ed.* **2014,** *126*, 13426-13430.

97. Chlubná, P.; Roth, W. J.; Zukal, A.; Kubů, M.; Pavlatová, J., *Catal. Today* **2012,** *179*, 35-42.

98. Eliášová, P.; Opanasenko, M.; Wheatley, P. S.; Shamzhy, M.; Mazur, M.; Nachtigall, P.; Roth, W. J.; Morris, R. E.; Čejka, J., *Chem. Soc. Rev.* **2015,** *44*, 7177-7206.

99. Trachta, M.; Nachtigall, P.; Bludský, O., *Catal. Today* **2015**, 32-38.

100. Gil, B.; Zones, S. I.; Hwang, S. J.; Bejblová, M.; Čejka, J., *Phys. Chem. C* **2008,** *112*, 2997-3007.

101. The DEPTH filter is a composite (90°-180°-180°) excitation pulse with 16-step phase cycling (onepuldpth Agilent pulse program) to suppress the background signal from the Kel-F spacers, adapted from Cory, D.G.; Ritchey, W.M. *J. Magn. Reson.* **1988**, *80*, 128.

102. Chlubná, P.; Roth, W. J.; Greer, H. F.; Zhou, W. Z.; Shvets, O.; Zukal, A.; Čejka, J.; Morris, R. E., *Chem. Mater.* **2013,** *25*, 542-547.

103. Kruk, M.; Jaroniec, M., *Chem. Mater.* **2001,** *13*, 3169-3183.

104. Položij, M.; Thang, H. V.; Rubeš, M.; Eliášová, P.; Čejka, J.; Nachtigall, P., *Dalton Trans.* **2014,** *43*, 10443-10450.

105. Sanders, M.; Leslie, M.; Catlow, C., *J. Am. Chem. Soc.* **1984,** *19*, 1271-1273.

7. Enclosures

1. M. Mazur, P.S. Wheatley, M. Navarro, W.J. Roth, M. Položij, A. Mayoral, P. Eliášová, P. Nachtigall, J. Čejka, R.E. Morris, *Synthesis of 'unfeasible' zeolites*, **Nature Chem.**, 8 (2016) 58-62

2. M. Mazur, P. Chlubná- Eliášová, W.J. Roth, J. Čejka, *Intercalation chemistry of layered zeolite precursor IPC-1P*, **Catal. Today**, 227 (2014) 37–44

3. M. Shamzhy, M. Mazur, M. Opanasenko, W.J. Roth, J. Čejka, *Swelling and pillaring of the layered precursor IPC-1P: tiny details determine everything*, **Dalton Trans.**, 43 (2014) 10548-10557

4. M. Mazur, M. Kubů, P.S. Wheatley, P. Eliášová, *Germanosilicate UTL and its rich chemistry of solid-state transformations towards IPC-2 (OKO) zeolite*, **Catal. Today**, 243 (2015) 23–31

5. P. Eliášová, M. Opanasenko, P.S. Wheatley, M. Shamzhy, M. Mazur, P. Nachtigall, W.J. Roth, R.E. Morris, J. Čejka, *The ADOR mechanism for the synthesis of new zeolites*, **Chem. Soc. Rev.**, 44 (2015) 7177-7206

6. M. Opanasenko, W. O. Parker Jr., M. Shamzhy , E. Montanari, M. Bellettato, M. Mazur, R. Millini, J. Čejka, *Hierarchical hybrid organic-inorganic materials with tunable textural properties obtained using zeolitic layered* precursor, **J. Am. Chem. Soc.**, 136 (2014) 2511–2519

7. R. L. Smith, P. Eliášová, M. Mazur, M. P. Attfield, J. Čejka, M. Anderson, *Atomic Force Microscopy of Novel Zeolitic Materials Prepared by Top-Down Synthesis and ADOR Mechanism*, **Chem. Eur. J.**, 20 (2014) 10446-1045

8. N. Žilková, P.Eliášová, S. Al-Khattaf, R.E. Morris, M. Mazur, J. Čejka, *The effect of UTL layer connectivity in isoreticular zeolites on the catalytic performance in toluene alkylation*, **Catal. Today**, in press, doi:10.1016/j.cattod.2015.09.033